

The pruritus- and T_H2-associated cytokine IL-31 promotes growth of sensory nerves

Micha Feld, PhD,^a Richard Garcia, PhD,^b Jörg Buddenkotte, PhD,^a Shintaro Katayama, PhD,^c Katherine Lewis, PhD,^b Gareth Muirhead, MSc,^d Peter Hevezi, PhD,^e Kristin Plessner, MSc,^a Holger Schruppf, MSc,^a Kaarel Krjutskov, PhD,^c Olga Sergeeva, PhD,^f Hans Werner Müller, PhD,^g Sophia Tsoka, PhD,^d Juha Kere, MD, PhD,^c Stacey R. Dillon, PhD,^b Martin Steinhoff, MD, PhD,^{a,h*} and Bernhard Homey, MD^{a*}
 Düsseldorf, Germany, Seattle, Wash, Huddinge, Sweden, London, United Kingdom, Irvine, Calif, and Dublin, Ireland

Background: Pruritus is a cardinal symptom of atopic dermatitis, and an increased cutaneous sensory network is thought to contribute to pruritus. Although the immune cell–IL-31–neuron axis has been implicated in severe pruritus during atopic skin inflammation, IL-31's neuroipoietic potential remains elusive.

Objective: We sought to analyze the IL-31–related transcriptome in sensory neurons and to investigate whether IL-31 promotes sensory nerve fiber outgrowth.

Methods: *In vitro* primary sensory neuron culture systems were subjected to whole-transcriptome sequencing, ingenuity pathway analysis, immunofluorescence, and nerve elongation, as well as branching assays after IL-31 stimulation. *In vivo* we investigated the cutaneous sensory neuronal network in wild-type, *IL31*-transgenic, and IL-31 pump–equipped mice.

Results: Transgenic *IL31* overexpression and subcutaneously delivered IL-31 induced an increase in the cutaneous nerve fiber density in lesional skin *in vivo*. Transcriptional profiling of IL-31–activated dorsal root ganglia neurons revealed enrichment for genes promoting nervous system development and neuronal outgrowth and negatively regulating cell death. Moreover, the growth cones of primary small-diameter dorsal root ganglia neurons showed abundant IL-31 receptor α expression. Indeed,

IL-31 selectively promoted nerve fiber extension only in small-diameter neurons. Signal transducer and activator of transcription 3 phosphorylation mediated IL-31–induced neuronal outgrowth, and pharmacologic inhibition of signal transducer and activator of transcription 3 completely abolished this effect. In contrast, transient receptor potential cation channel vanilloid subtype 1 channels were dispensable for IL-31–induced neuronal sprouting.

Conclusions: The pruritus- and T_H2-associated novel cytokine IL-31 induces a distinct transcriptional program in sensory neurons, leading to nerve elongation and branching both *in vitro* and *in vivo*. This finding might help us understand the clinical observation that patients with atopic dermatitis experience increased sensitivity to minimal stimuli inducing sustained itch. (J Allergy Clin Immunol 2016;■■■■:■■■■-■■■■.)

Key words: IL-31, IL-31 receptor α , dorsal root ganglia, atopic dermatitis, nerve growth, cutaneous hyperinnervation

From ^athe Department of Dermatology, University Hospital Düsseldorf; ^bZymoGenetics (a Bristol-Myers Squibb Company), Seattle; ^cthe Department of Biosciences and Nutrition, Karolinska Institutet, Huddinge; ^dthe Department of Informatics, King's College London; ^ePhysiology and Biophysics, University of California, Irvine; ^fthe Department of Neurophysiology and ^gthe Molecular Neurobiology Laboratory, Neurology, Heinrich Heine University, Düsseldorf; and ^hthe Department of Dermatology and UCD Charles Institute for Translational Dermatology, Dublin.

*These authors contributed equally to this work.

Supported by the European Union's Seventh Framework Programme FP7/2007-2013 under grant agreement no. 261366 (to B.H.), the SFI IVP award, National Institutes of Health (AR059402-01A1)/National Institute of Arthritis and Musculoskeletal and Skin Diseases grant R01 (AR059402), Toray Japan, and the Skin and Cancer Hospital Charity Dublin (to M.S.).

Disclosure of potential conflict of interest: R. Garcia declares he is an employee of and received travel funding from Bristol-Myers Squibb. K. Lewis declares she is an employee and stockholder of receives travel funding from Bristol-Myers Squibb. S. R. Dillon is an employee of and stockholder in and receives travel funding from Bristol-Myers Squibb. M. Steinhoff declares that he has received grants from SFI IVP, the Debra Foundation, and the City of Dublin Skin Cancer Hospital Charity. The rest of the authors declare that they have no relevant conflicts of interest.

Received for publication July 14, 2015; revised January 25, 2016; accepted for publication February 4, 2016.

Corresponding author: Bernhard Homey, MD, Department of Dermatology, University Hospital Düsseldorf, Moorenstrasse 5, 40225 Düsseldorf, Germany. E-mail: bernhard.homey@uni-duesseldorf.de.

0091-6749/\$36.00

© 2016 American Academy of Allergy, Asthma & Immunology

<http://dx.doi.org/10.1016/j.jaci.2016.02.020>

In patients with atopic dermatitis (AD), a chronic T_H2-dominated inflammatory skin disease, pruritus is the cardinal symptom with the most significant adverse effect on patients' quality of life and high socioeconomic costs.^{1,2} Physical and psychological stress responses in patients with AD³ and T_H2 cytokine–related skin barrier defects⁴ might promote the pruritus sensation. Development of chronic pruritus relies not only on increased availability of itch mediators but also most likely takes advantage of increased density of cutaneous neuronal networks with prolonged sensory nerve fibers extending into the epidermal compartment.⁵⁻⁷ Moreover, the diameter of these fibers appears to be thicker in skin of patients with AD because of an increased number of axons on single nerve fibers.⁸ Phenotypic characterization of cutaneous nerve fibers reveals an increased number of substance P–positive and/or calcitonin gene-related protein–positive nerve fibers in the skin of atopic subjects.⁹⁻¹¹ Several reports have proposed a role for neurotrophins, cytokines, or both in AD-associated cutaneous nerve growth.^{11,12} However, the mechanism that controls sensory nerve fiber growth in patients with atopic skin inflammation and that might contribute to the typical pruritic hypersensitivity of patients with AD still remains elusive.

The novel atopy-associated cytokine IL-31 plays a crucial role in AD, asthma, allergic rhinitis, and mastocytosis.¹³⁻¹⁵ IL-31 belongs to the IL-6 family of cytokines¹⁶ and is mainly, but not exclusively, produced by activated T_H2 cells.^{17,18} Transcription of the *IL31* gene in T_H2 and mast cells requires IL-4 signaling.¹⁹ The IL-31 receptor subunits IL-31 receptor α (IL-31RA) and oncostatin M receptor β are coexpressed on sensory neurons,^{20,21} and recent evidence indicates that IL-31 from skin-infiltrating

Abbreviations used

AD:	Atopic dermatitis
DRG:	Dorsal root ganglia
ERK:	Extracellular signal-regulated kinase
IL-31RA:	IL-31 receptor α
IPA:	Ingenuity pathway analysis
NGF:	Nerve growth factor
PGP9.5:	Protein gene product 9.5
PI3K:	Phosphoinositide 3-kinase
<i>Prph</i> :	Peripherin gene
RNA-Seq:	RNA sequencing
STAT3:	Signal transducer and activator of transcription 3
STRT:	Single cell–tagged reverse transcription
Tg:	Transgenic
TrkA:	Tropomyosin receptor kinase A
TRPV1:	Transient receptor potential cation channel vanilloid subtype 1

T_H2 lymphocytes can communicate with sensory neurons, thereby triggering the development of pruritus and skin lesions in mice.^{17,18,22,23} Skin areas devoid of T-lymphocyte infiltration are not affected by IL-31 signaling. Indeed, in patients with AD, IL-31 provides a novel link connecting *Staphylococcus*-related T-cell activation and pruritus.²⁰

We reported recently that IL-31–induced pruritus in mice requires functional ion channels, namely transient receptor potential cation channel vanilloid subtype 1 (TRPV1) and transient receptor potential A1, on cutaneous sensory neurons and that this process is uncoupled from mast cells.¹⁸ Moreover, pharmacologic inhibition of extracellular signal-regulated kinase (ERK1/2) signaling hampers IL-31–mediated pruritus.¹⁸ However, neither immunosuppressants nor μ -opioid receptor or a histamine H₁ antagonist alleviate pruritus elicited by exogenous IL-31.²⁴ In contrast, in mice with chronic atopy-like skin inflammation, itch-scratch cycles are significantly reduced by administration of neutralizing anti-IL-31 or anti-IL-31RA antibodies.^{22,24} Intriguingly, a recent clinical phase I trial in patients with AD using a humanized mAb targeting IL-31RA demonstrated significant improvement of pruritus,²⁵ providing further evidence that IL-31 links T_H2-related inflammation to pruritus.

Although the T_H2 cell–IL-31–sensory neuron axis and its role in pruritus are now well established, the question of whether IL-31 is also involved in the increased density of sensory networks within the skin remains elusive.

METHODS**Mice and sample collection**

Six to 8-week-old wild-type C57BL/6, *Il31ra*, and *Trpv1* knockout mice were kept under specific pathogen-free conditions. *Il31* transgenic (Tg) mice specifically overexpressing *Il31* under the E μ -Lck promoter in lymphocytes¹⁷ and control littermates were housed for up to 9 months under specific pathogen-free conditions until characteristic lesions developed spontaneously. For further details, see the **Methods** section in this article's Online Repository at www.jacionline.org.

Preparation and treatment of dorsal root ganglia neurons

Adult C57BL/6 mice and *Il31ra* knockout mice were killed and DRGs from the lumbar, thoracic, and cervical regions were removed to prepare sensory

neurons from dissociated dorsal root ganglia (DRG) neurons. For further details, see the **Methods** section in this article's Online Repository.

Immunofluorescence and image analysis

OCT-embedded skin samples were cut in 20- μ m-thick sections to analyze cutaneous innervation. For further details, see the **Methods** section in this article's Online Repository.

RNA sequencing and data analysis

The single cell–tagged reverse transcription (STRT) method was used²⁶ with minor modifications to measure transcription initiation at the 5' end of polyA⁺ transcripts starting from 10 ng of total RNA as template. For further details, see the **Methods** section in this article's Online Repository.

Western blotting

Proteins from IL-31–activated DRG neurons were harvested with Roti-Load buffer (Carl Roth, Karlsruhe, Germany) supplemented with 2-mercaptoethanol at the indicated time points and boiled for 10 minutes. For further details, see the **Methods** section in this article's Online Repository.

Quantitative real-time PCR

RNA was prepared from IL-31– and nerve growth factor (NGF)–activated DRG neurons with the RNeasy kit (Qiagen, Hilden, Germany) and reverse transcribed with SuperScript II (Invitrogen, Carlsbad, Calif), according to the manufacturer's instructions. For further details, see the **Methods** section in this article's Online Repository.

Statistical analysis

Results are expressed as means \pm SEMs. At least 3 independent experiments were conducted ($n \geq 3$). Statistical analysis was performed with GraphPad Prism 5 software (GraphPad software, La Jolla, Calif). Significance was evaluated by using the paired *t* test, Mann-Whitney test, Wilcoxon matched-pairs signed-rank test, and 1-way ANOVA with *post hoc* Tukey, Newman-Keuls, or Dunnett tests. Significance was set at a *P* value of less than .05.

RESULTS**Transgenic overexpression of *Il31* results in increased cutaneous innervation**

IL-31 is associated with AD and directly activates peripheral sensory neurons to induce pruritus.¹⁸ Patients with AD with chronic pruritus show increased cutaneous innervation.⁵ To unravel an additional role for IL-31 in cutaneous innervation, we took advantage of *Il31*Tg mice, which have an AD-like skin phenotype with severe pruritus spontaneously affecting the nape of the neck and ears (Fig 1, A, and see Fig E1 in this article's Online Repository at www.jacionline.org). First, we characterized the nerve fiber density in lesional and nonlesional skin from *Il31*Tg mice¹⁷ and healthy skin from wild-type littermates (Fig 1, B) by using immunofluorescence to visualize protein gene product 9.5 (PGP9.5)⁺ nerve fibers. Our results demonstrated that *Il31*Tg mice show a marked and significant increase in the cutaneous nerve fiber density in lesional skin (8.5 ± 2.7 PGP9.5⁺ fibers, $P < .01$) compared with that in uninvolved or healthy skin (*Il31*Tg nonlesional: 0.75 ± 0.4 PGP9.5⁺ fibers or healthy C57BL/6 wild-type: 0.42 ± 0.2 PGP9.5⁺ fibers; Fig 1, B and C). Expression of the DRG neuron-specific transcript peripherin gene (*Prph*) is increased in the skin of *Il31*Tg mice (see Fig E2, G, in this article's Online Repository at

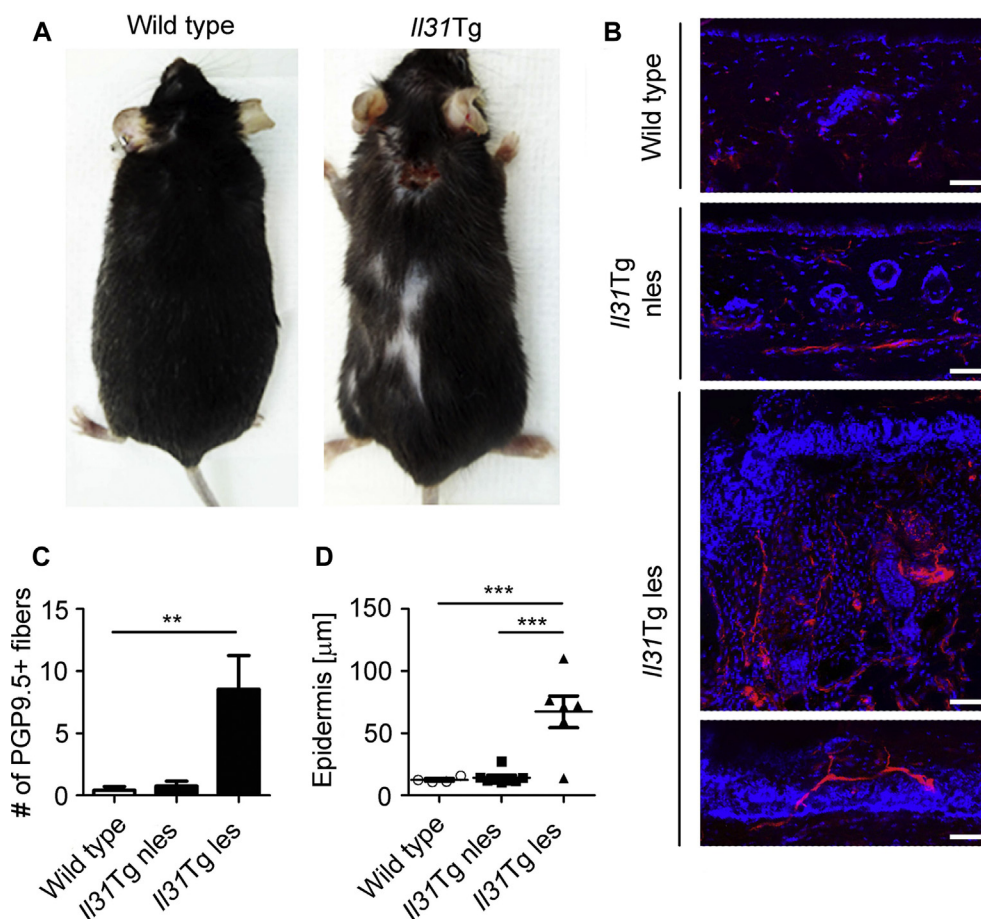


FIG 1. Skin innervation is dysregulated in *Il31* transgenics. **A**, Development of pruritic skin lesions in the nape of the neck during conventional housing. **B**, Immunofluorescence of PGP9.5⁺ nerve fibers in *Il31Tg* skin and wild-type littermates (epidermis oriented upward). **C**, Quantification of cutaneous PGP9.5⁺ nerve fibers. **D**, Measurement of epidermal thickening. ** $P < .01$ and *** $P < .001$, ANOVA with Tukey or Dunnett *post hoc* testing.

www.jacionline.org). Moreover, *Il31Tg* lesional skin shows significantly increased epidermal thickening ($67.2 \pm 31.2 \mu\text{m}$, $P < .001$) compared with uninvolved skin (Fig 1, D). To further substantiate our findings, we investigated changes in the cutaneous nerve fiber density in BALB/c mice supplemented with an iso-osmotic pump dispensing mIL-31 for 14 days subcutaneously and in naive BALB/c mice. We found that continuous delivery of exogenous mIL-31 promotes development of AD-like skin lesions, pruritus/scratching, and hair loss starting from day 6 onward (see Fig E3, D, in this article's Online Repository at www.jacionline.org). Lesional skin from IL-31-treated BALB/c mice is hyperinnervated compared with nonlesional skin and skin from naive, healthy BALB/c mice (see Fig E3, A and B), and the abundance of the DRG neuron-specific transcript *Prph* is enhanced in lesional skin from mIL-31-treated BALB/c mice (see Fig E3, E). Moreover, IL-31 increases epidermal thickening in BALB/c mice (see Fig E3, C).

IL-31 induces distinct genes related to neuronal growth in primary DRG neurons

To further study IL-31's neurotrophic potential and to compare its function with the well-characterized neurotrophin NGF, we

analyzed their transcriptional profiles using RNA sequencing (RNA-Seq; see Fig E4 in this article's Online Repository at www.jacionline.org). First, we found that IL-31 and NGF significantly upregulate 259 and 216 genes in dissociated DRG neurons, respectively. Notably, only 31 genes were shared between these treatment conditions (Fig 2, A). Surprisingly, very few genes were downregulated (6 by IL-31 and 12 by NGF), suggesting that both factors activate DRG neurons (Fig 2, A). To validate the IL-31 data set, 6 randomly selected upregulated genes (*Il31ra*, *Shroom3*, *Nts*, *Rcan1*, *Sema6D*, and *Cyth2*) were analyzed in biological replicates ($n = 4-5$), and 5 of 6 genes were significantly induced by IL-31 (see Fig E2), supporting the reliability of the RNA-Seq data set.

Next, differentially expressed genes were annotated and assigned to functional biological classes. Although upregulating different gene sets, both IL-31- and NGF-related genes belong to the same functional classes, such as cell morphology/adhesion, gene expression, (protein) metabolism, neuronal, and transport(er) (Fig 2, B). Moreover, ingenuity pathway analysis (IPA) revealed that 7 of the 10 most significantly enriched pathways are shared between IL-31- and NGF-activated neurons (eukaryotic translation initiation factor 2 signaling, oxidative phosphorylation, gluconeogenesis I, mitochondrial dysfunction, unfolded

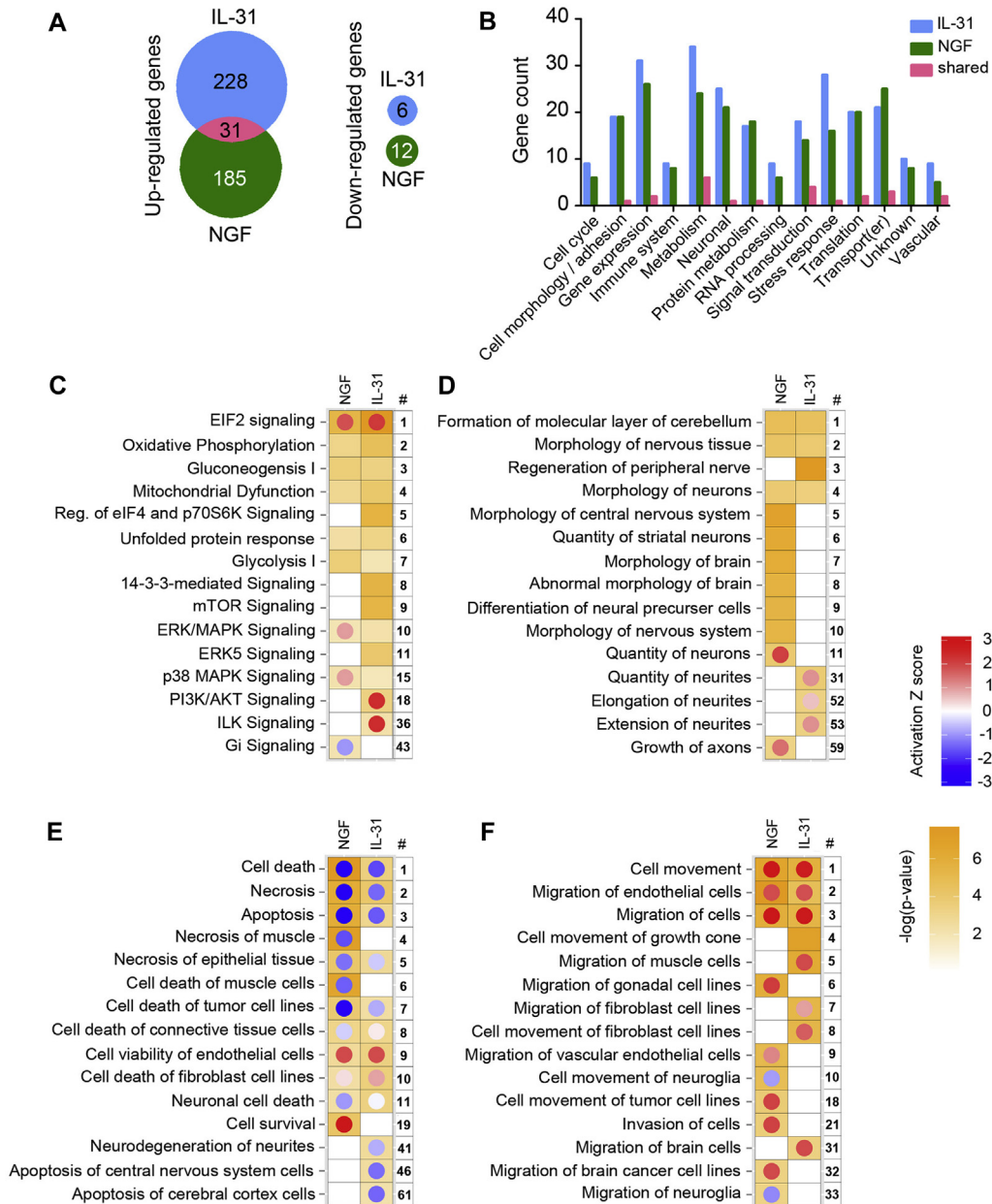


FIG 2. mIL-31- and NGF-induced genes relate to similar biological processes but upregulate different sets of genes. **A**, Differential gene expression profiles in stimulated and dissociated DRG neurons. **B**, Functional annotations of IL-31- and NGF-induced genes. **C**, Chart showing signaling pathways related to IL-31 and NGF activation of DRG neurons. **D-F**, Charts showing enrichment of functional annotations in the categories of nervous system development (Fig 2, D), cell death and survival (Fig 2, E), and cellular movement (Fig 2, F). The activation z score indicates the direction of regulation: positive (score > 1) and negative (score < -1). *EIF2*, Eukaryotic translation initiation factor 2; *ILK*, integrin-linked kinase; *MAPK*, mitogen-activated protein kinase. #Number of enriched molecules.

protein response, glycolysis I, and ERK/mitogen-activated protein kinase signaling; Fig 2, C). However, IPA also identified enrichment of signaling pathways specific for IL-31 (eg, 14-3-3 signaling, mechanistic target of rapamycin signaling, phosphoinositide 3-kinase [PI3K]/AKT signaling, and integrin-linked kinase signaling) or NGF (eg, Gi signaling, cyclic AMP-mediated signaling, and cholesterol biosynthesis I; see Fig E4 in this article's Online Repository at www.jacionline.org). Interestingly, IPA indicated that differentially expressed genes

associated with either IL-31 or NGF stimulation are related to a variety of functional annotations within 3 central categories: nervous system development (Fig 2, D), cell death and survival (Fig 2, E), and cellular movement (Fig 2, F). In these categories IL-31- and NGF-induced gene sets not only promote overlapping biological responses but also relate to different functional annotations. However, if linked to different functional annotations, the IL-31- and NGF-activated genes can be assigned to similar biological functions promoting neuronal growth

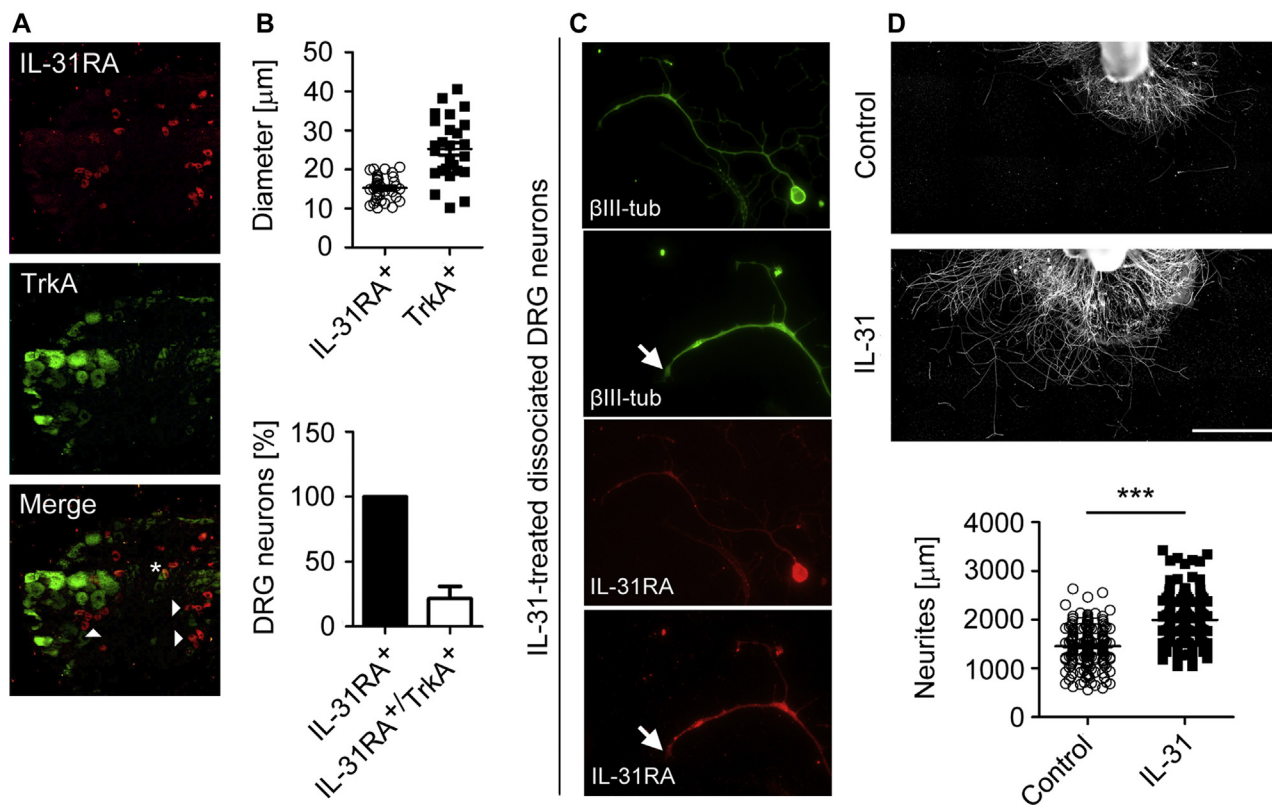


FIG 3. IL-31RA is expressed on small-diameter neurons, and mIL-31 promotes axonal growth in DRG explants. **A**, Colocalization of IL-31RA and TrkA (NGF receptor) in DRG sections. *Colocalization of IL-31RA with TrkA. **B**, The minority of IL-31RA⁺ small-diameter DRG neurons coexpress TrkA. **C**, Identification of IL-31RA in growth cones of DRG neurons. **D**, mIL-31-induced neuronal sprouting in DRG explants. *** $P < .001$, Mann-Whitney test.

(regeneration of peripheral nerve, neuronal outgrowth, and cell survival; see Fig E4) and cell movement (Fig 2, F). Indeed, within the category of nervous system development, IL-31 positively regulates the quantity of neurites and the extension of neurites, whereas NGF induces genes positively regulating the quantity of neurons and growth of axons (activation z score > 1 ; Fig 2, D). In contrast, activation of functions like necrosis, apoptosis, and cell death is negatively regulated in response to both IL-31 and NGF (activation z score < -1 ; Fig 2, E).

IL-31 promotes neuronal growth in small-diameter neurons

To analyze the distribution pattern and coexpression of IL-31RA and tropomyosin receptor kinase A (TrkA; the specific NGF receptor) in neuron subsets, we performed immunofluorescence staining on primary DRG neurons isolated from wild-type mice. We found that IL-31RA is expressed only on small-diameter neurons (diameter, $< 20 \mu\text{m}$), whereas TrkA is found on small- and large-diameter (diameter, $> 20 \mu\text{m}$) neurons (Fig 3, A and B, upper panel). Only $21\% \pm 9\%$ of all IL-31RA⁺ DRG neurons also stain positive for TrkA (Fig 3, B, lower panel). Moreover, in IL-31-activated DRG neurons, IL-31RA is located in the growth cones and cell bodies (Fig 3, C). To further investigate the role of IL-31 in neuronal outgrowth, whole DRG explants from wild-type mice ($n = 6$) were stimulated with IL-31 or control ($n = 19$ DRGs per condition), and the length

of the 10 longest neurites per DRG was measured. Interestingly, stimulation of whole DRG explants with IL-31 for 3 days leads to (1) increased neuronal growth and (2) neurite elongation (Fig 3, D). Quantitation of the length of the 10 longest neurites per DRG explant revealed that IL-31 significantly promotes nerve fiber elongation ($1993 \pm 33.6 \mu\text{m}$, $P < .0001$) compared with control values ($1458 \pm 28.6 \mu\text{m}$; Fig 3, D). To further validate the finding that only small-diameter neurons are responsive to IL-31, we used cultured dissociated DRG neurons ($n = 43$ –58 neurons per condition in 5 independent experiments) to measure the diameter of each neuron and to treat these neurons with IL-31, NGF, or vehicle control for 24 hours. In dissociated DRG neurons with a small diameter ($< 20 \mu\text{m}$), we found that both IL-31 ($318.1 \pm 17.9 \mu\text{m}$, $P < .001$) and NGF ($325 \pm 27.8 \mu\text{m}$, $P < .01$) induce nerve fiber elongation compared with control neurons ($220.6 \pm 14.2 \mu\text{m}$; Fig 4, A and B). Interestingly, in contrast to NGF, IL-31 also promoted increased branching of the longest neurites extending from small-diameter neurons prepared from wild-type mice ($< 20 \mu\text{m}$, $P = .01$; Fig 4, C). In large-diameter neurons ($> 20 \mu\text{m}$) only NGF, but not IL-31, affected nerve fiber elongation (Fig 4, D). To confirm that IL-31 biology is mediated by its specific receptor IL-31RA, we prepared dissociated DRG neurons derived from *Il31ra*-deficient mice. In contrast to wild-type mice, IL-31 did not augment neuronal elongation and branching of small-diameter neurons of *Il31ra*^{-/-} mice ($207 \pm 14.1 \mu\text{m}$) when compared with untreated control mice ($178.5 \pm 21.5 \mu\text{m}$; Fig 4, E and F).

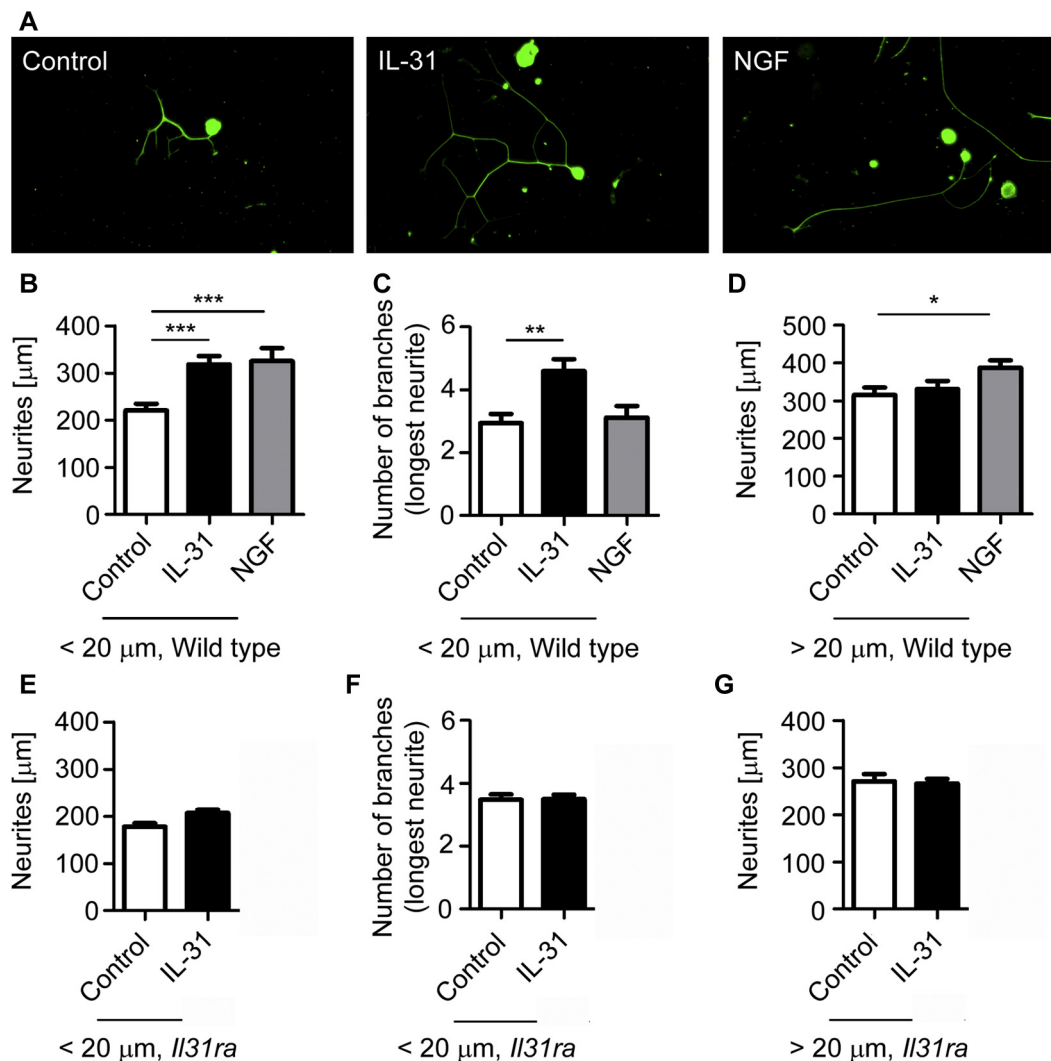


FIG 4. mIL-31 induces neuronal outgrowth and branching in small-diameter neurons. **A**, Outgrowth of sensory nerve fibers in wild-type DRG cultures. **B** and **C**, Quantification of the neurite length (Fig 4, **B**) and branching (Fig 4, **C**) in small-diameter wild-type DRG neurons. **D**, Quantification of the neurite length in large-diameter wild-type DRG neurons. **E** and **F**, Quantification of the neurite length (Fig 4, **E**) and branching (Fig 4, **F**) in *Il31ra*^{-/-} small-diameter DRG neurons. **G**, Quantification of the neurite length in *Il31ra*^{-/-} large-diameter DRG neurons. * $P < .05$, ** $P < .01$, and *** $P < .001$, ANOVA with Tukey or Newman-Keuls *post hoc* testing.

Signal transducer and activator of transcription 3 phosphorylation links IL-31 and nerve fiber elongation

To identify the signaling pathway involved in IL-31-related neuronal growth in DRG neurons, we first studied the IL-31-mediated phosphorylation of ERK1/2 and signal transducer and activator of transcription 3 (STAT3) using Western blotting. We found that IL-31 triggers both ERK1/2 ($P < .05$) and STAT3 ($P < .05$) phosphorylation in dissociated DRG neurons ($n = 6$ independent experiments; Fig 5, **A-C**). Because STAT3 is a common mediator of neuronal growth response,²⁷ we analyzed whether IL-31 uses STAT3 signaling to promote neurite elongation using the STAT3-specific inhibitor Stattic in DRG neurons. Pretreatment of DRG neurons with Stattic significantly abolished IL-31-induced neurite elongation in both dissociated neurons ($P < .0001$; $n = 75-85$ neurons per condition in 4

independent experiments; Fig 5, **D**) and whole DRG explants ($P < .001$; $n = 12$ DRGs per condition in 3 independent experiments; Fig 5, **E**) compared with vehicle-treated control values. Moreover, we showed that Stattic decreases basal nerve fiber elongation in the control compared with dimethyl sulfoxide-treated control ($P < .001$; Fig 5, **E**).

IL-31-induced nerve fiber elongation is independent of TRPV1

Previously, we demonstrated that IL-31-induced pruritus requires active TRPV1 channels.¹⁸ Thus we further aimed to determine the contribution of TRPV1 to IL-31-induced neurite outgrowth. Using *Trpv1*-deficient mice, we showed that IL-31 promotes neurite outgrowth independently of TRPV1 ($n = 16-20$ DRGs per condition in 3 independent experiments; Fig 5, **F**).

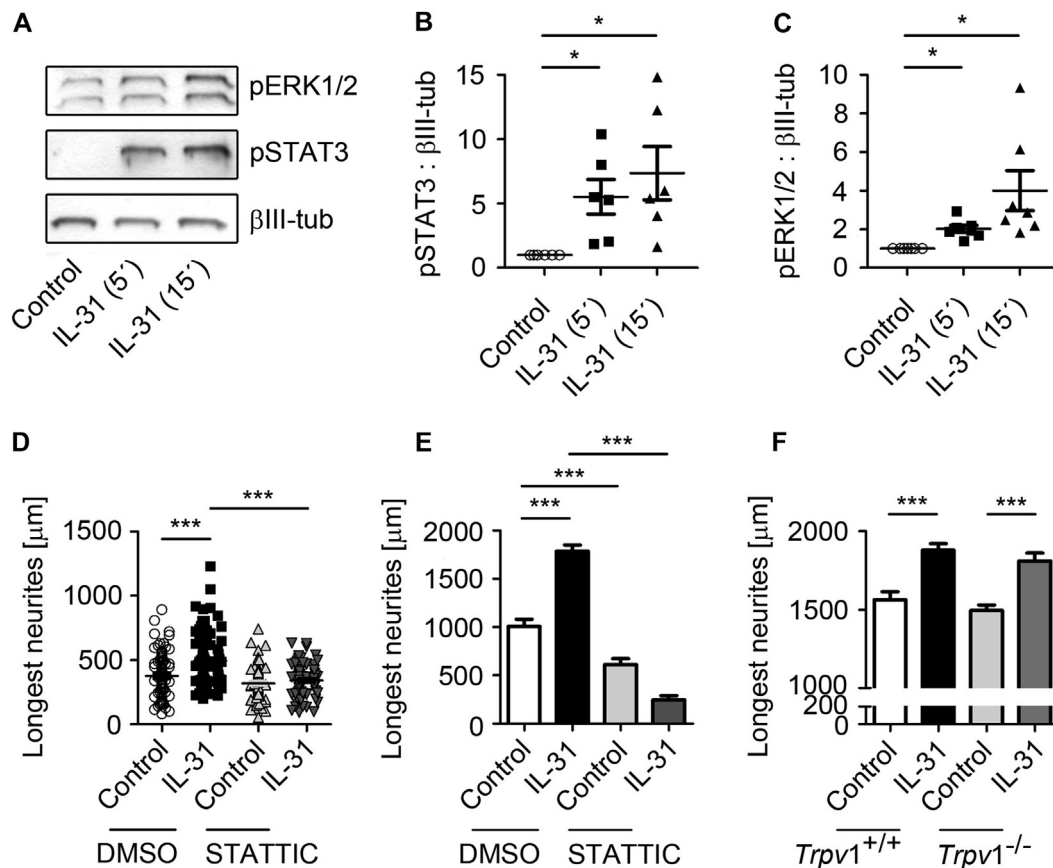


FIG 5. mIL-31-activated STAT3 signaling regulates neurite elongation in DRG neurons. **A–C,** Quantitation of mIL-31-induced ERK1/2 and STAT3 phosphorylation in DRG neurons. **D and E,** Stattic-related outgrowth inhibition in dissociated DRG neurons (Fig 5, D) and DRG explants (Fig 5, E). **F,** Quantitation of outgrowth in *Trpv1*^{-/-} neurons. **P* < .05 and ****P* < .001, Wilcoxon matched-pairs signed-rank test, ANOVA with Tukey *post hoc* testing. *DMSO*, Dimethyl sulfoxide.

DISCUSSION

In patients with AD, agonizing itch sensation involves an increased density of cutaneous sensory nerve fibers.⁵ Current concepts implicate an imbalance of neurotrophins and repulsive factors as participating in pruritus-associated pathology.⁶ Because AD represents a chronic inflammatory disease, a role for T_H2 cytokines in promoting the elongation of sensory nerves during atopic skin inflammation has also been proposed.¹² Here, for the first time in a murine model, we report that the T_H2-related and atopy-associated cytokine IL-31 directly promotes nerve fiber elongation *in vitro* and *in vivo* (Figs 1, 3, and 4). Moreover, we demonstrate that IL-31 increases neurite branching in activated DRG neurons (Fig 4, C). Intriguingly, AD-related factors, such as IL-4 and staphylococcal enterotoxin B, augment IL-31 production in human subjects,^{20,28} suggesting that endogenous and/or environmental triggers might engage the IL-31 pathway to promote cutaneous innervation in atopic subjects. Indeed, transcriptional profiling of IL-31-activated DRG neurons from mice further supports a neuropoietic function of IL-31. Pathway analysis revealed enrichment for pathways related to neurogenesis in general and to neurite branching and elongation of neurites in particular (Fig 2, D, and see the Methods section in this article's Online Repository). Interestingly, IPA indicated an IL-31-induced innervation of the skin response (see Fig E4). Moreover,

our findings are also supported by initial correlative findings by Murota et al.²⁹ IL-31 has been assigned to the IL-6 family of cytokines,¹⁶ which emerged as a cytokine family with dual functions: inflammation and neuropoiesis.³⁰ The IL-6 family members leukemia inhibitory factor, ciliary neurotrophic factor, and oncostatin M regulate nervous system development, neuronal survival, or repair^{30–34} through a selective receptor heterodimer specific for each IL-6 family member. However, unlike all other IL-6 family-related receptor heterodimers, the IL-31 receptor complex uses a unique gp130-like receptor chain IL-31RA.¹⁶ Our recent studies revealed that IL-31RA is expressed exclusively on a subset of small-diameter neurons (<20 μm; Fig 3, A) of TRPV1⁺ peptidergic murine DRG neurons, which evokes profound scratching in mice through an ERK1/2-dependent mechanism.¹⁸ The clinical relevance of these findings is supported by the positive results of a recent clinical study using a neutralizing anti-IL-31RA mAb to control pruritus in patients with AD.²⁵ Here we demonstrate that IL-31RA is targeted to the growth cones of primary sensory neurons (Fig 3, C), further suggesting an essential role for IL-31 in neuron-growth cone guidance, as demonstrated previously for other neurotrophins.^{35,36}

Previously, the dysregulation of NGF and semaphorin 3A was proposed to explain how increased cutaneous sensory nerve

density is regulated in patients with AD.⁶ In this model keratinocyte-derived NGF is one of the mediators determining the innervation density in skin of patients with AD, which is characterized by decreased levels of the repulsive axon guidance factor semaphorin 3A.^{37,38} Nonetheless, current evidence suggests that additional T_H2 inflammation-related mechanisms are triggering skin innervation and scratching behavior in mice with chronic AD.¹² Although intradermal injection of mIL-31 induces intense immediate pruritus in mice,¹⁸ Hawro et al²³ reported that skin prick testing with human IL-31 only induced delayed pruritus (9/20 subjects) 2 hours after injection. Hence further research will be necessary to investigate how IL-31 directly or indirectly communicates with neurons to cause pruritus in human subjects.

In the present study we extend our understanding of the neuronal function of IL-31 promoting the elongation of IL-31RA⁺ neurons (Figs 3, D, and 4). Immunofluorescence analysis of IL-31RA⁺ neurons further revealed that only the minority of IL-31-responsive neurons coexpresses TrkA (Fig 3, A and B), proposing that IL-31 elongates a unique subset of itch-conducting sensory nerve fibers that are unresponsive to NGF. To further characterize the differences/similarities between IL-31- and NGF-induced nerve fiber out growth, we compared the transcriptional profiles of murine DRG neurons cultured with IL-31 or NGF by means of whole-transcriptome sequencing. Intriguingly, although IL-31 and NGF enrich genes that relate to similar biological processes, the transcriptional profile is quite different (Fig 2), suggesting that both agonists might activate different neurons. IL-31 stimulation leads to enrichment of signaling pathways linked to nervous system development and survival: PI3K/AKT, mitogen-activated protein kinase, mammalian target of rapamycin, and 14-3-3 signaling.³⁹⁻⁴² Interestingly, pathways enriched and positively regulated in response to IL-31, like PI3K/AKT and integrin-linked kinase signaling, trigger peripheral axon regeneration,⁴³ axonal elongation,⁴¹ and neuronal polarity.⁴⁴ STAT3 was identified as (1) an important positive regulator of peripheral nerve regeneration and neuronal outgrowth^{27,45} and (2) a protective factor rescuing from axonal degeneration,⁴⁶ thus strongly suggesting a role for STAT3 in IL-31-related nerve fiber growth responses. These findings are supported by IL-31-induced STAT3 phosphorylation in murine neurons (Fig 5, A and B) and the fact that pharmacologic inhibition of the STAT3 pathway completely abolishes IL-31-mediated neuron outgrowth (Fig 5, D and E). Interestingly, it has been reported recently that NGF requires basal activity of the IL-6 family receptor-related gp130 to induce STAT3 phosphorylation and to promote neuronal outgrowth in DRG neurons,⁴⁵ suggesting that both IL-31 and NGF promote nerve fiber elongation through STAT3 phosphorylation but target different neuron subsets. Recently, we could demonstrate that IL-31-induced itch sensation in mice critically depends on ERK1/2 and functional TRPV1 channels.¹⁸ Although previous studies associated *Trpv1* with neurogenesis,⁴⁷ our findings in TRPV1-deficient mice show that IL-31-induced sensory neuron elongation and branching were independent of TRPV1 engagement (Fig 5, F). Hence these results suggest that one stimulus, IL-31, uses different signaling traits to evoke distinct downstream phenotypes.

In patients with AD, intractable pruritus causes severe clinical challenges and relies, on the activation of the IL-31 axis, among other factors. Based on previous findings and the results of the present study, we suggest the following model for the role of the

IL-31 axis in the skin. First, during atopic skin inflammation, immune cells, such as T_H2 cells, mast cells, or both, communicate with cutaneous IL-31RA⁺ sensory neurons through IL-31 secretion and induce itch sensations. Second, subsequently, chronic IL-31-driven “atopic” stimulation of cutaneous sensory neurons can result in cutaneous sensory nerve fiber elongation and branching, leading to increased sensory nerve fiber density in patients with AD. Third, given the enhanced sensory network within the skin, it is conceivable that itch thresholds are decreasing and that minimal doses of pruritogens can result in triggering symptoms in atopic subjects.

Taken together, because of its role in inflammation, itch, and nerve elongation, therapeutic targeting of the IL-31/IL-31RA pathway might be an attractive approach to break vicious itch-scratch-eczema cycles and to improve the patient’s quality of life.

We thank Michaela Fastrich for expert technical assistance. The computations were performed with resources provided by SNIC through Uppsala Multidisciplinary Center for Advanced Computational Science (UPPMAX) under Project b2014069.

Key messages

- The pruritus- and T_H2-associated novel cytokine IL-31 induces a distinct transcriptional program in sensory neurons.
- IL-31 induces the outgrowth of sensory neurons in a STAT3-dependent manner.
- Translational effect: IL-31-associated nerve elongation might be involved in skin hypersensitivity of patients with AD to pruritogenic trigger factors.

REFERENCES

1. Bieber T. Atopic dermatitis. *N Engl J Med* 2008;358:1483-94.
2. Eyerich K, Novak N. Immunology of atopic eczema: overcoming the Th1/Th2 paradigm. *Allergy* 2013;68:974-82.
3. Hamilton JD, Suárez-Fariñas M, Dhingra N, Cardinale I, Li X, Kostic A, et al. Dupilumab improves the molecular signature in skin of patients with moderate-to-severe atopic dermatitis. *J Allergy Clin Immunol* 2014;134:1293-300.
4. Kabashima K. New concept of the pathogenesis of atopic dermatitis: interplay among the barrier, allergy, and pruritus as a trinity. *J Dermatol Sci* 2013;70:3-11.
5. Cevikbas F, Steinhoff A, Homey B, Steinhoff M. Neuroimmune interactions in allergic skin diseases. *Curr Opin Allergy Clin Immunol* 2007;7:365-73.
6. Tominaga M, Takamori K. Itch and nerve fibers with special reference to atopic dermatitis: therapeutic implications. *J Dermatol* 2014;41:205-12.
7. Emtestam L, Hagströmer L, Dou YC, Sartorius K, Johansson O. PGP 9.5 distribution patterns in biopsies from early lesions of atopic dermatitis. *Arch Dermatol Res* 2012;304:781-5.
8. Urashima R, Mihara M. Cutaneous nerves in atopic dermatitis. A histological, immunohistochemical and electron microscopic study. *Virchows Arch* 1998;432:363-70.
9. Pincelli C, Fantini F, Massimi P, Girolomoni G, Seidenari S, Giannetti A. Neuropeptides in skin from patients with atopic dermatitis: an immunohistochemical study. *Br J Dermatol* 1990;122:745-50.
10. Järvikallio A, Harvima IT, Naukkarinen A. Mast cells, nerves and neuropeptides in atopic dermatitis and nummular eczema. *Arch Dermatol Res* 2003;295:2-7.
11. Ikoma A, Steinhoff M, Ständer S, Yosipovitch G, Schmelz M. The neurobiology of itch. *Nat Rev Neurosci* 2006;7:535-47.
12. Oh MH, Oh SY, Lu J, Lou H, Myers AC, Zhu Z, et al. TRPA1-dependent pruritus in IL-13-induced chronic atopic dermatitis. *J Immunol* 2013;191:5371-82.
13. Liu W, Luo R, Chen Y, Sun C, Wang J, Zhou L, et al. Interleukin-31 promotes helper T cell type-2 inflammation in children with allergic rhinitis. *Pediatr Res* 2015;77:20-8.

14. Lei Z, Liu G, Huang Q, Lv M, Zu R, Zhang GM, et al. SCF and IL-31 rather than IL-17 and BAFF are potential indicators in patients with allergic asthma. *Allergy* 2008;63:327-32.
15. Hartmann K, Wagner N, Rabenhorst A, Pflanz L, Leja S, Förster A, et al. Serum IL-31 levels are increased in a subset of patients with mastocytosis and correlate with disease severity in adult patients. *J Allergy Clin Immunol* 2013;132:232-5.
16. Cornelissen C, Lüscher-Firzlauff J, Baron JM, Lüscher B. Signaling by IL-31 and functional consequences. *Eur J Cell Biol* 2012;91:552-66.
17. Dillon SR, Sprecher C, Hammond A, Bilsborough J, Rosenfeld-Franklin M, Prensell SR, et al. Interleukin 31, a cytokine produced by activated T cells, induces dermatitis in mice. *Nat Immunol* 2004;5:752-60.
18. Cevikbas F, Wang X, Akiyama T, Kempkes C, Savinko T, Antal A, et al. A sensory neuron-expressed IL-31 receptor mediates T helper cell-dependent itch: involvement of TRPV1 and TRPA1. *J Allergy Clin Immunol* 2014;133:448-60.
19. Park K, Park JH, Yang WJ, Lee JJ, Song MJ, Kim HP. Transcriptional activation of the IL31 gene by NFAT and STAT6. *J Leukoc Biol* 2012;91:245-57.
20. Sonkoly E, Muller A, Lauerma AI, Pivarcsi A, Soto H, Kemeny L, et al. IL-31: a new link between T cells and pruritus in atopic skin inflammation. *J Allergy Clin Immunol* 2006;117:411-7.
21. Kato A, Fujii E, Watanabe T, Takashima Y, Matsushita H, Furuhashi T, et al. Distribution of IL-31 and its receptor expressing cells in skin of atopic dermatitis. *J Dermatol Sci* 2014;74:229-35.
22. Grimstad O, Sawanobori Y, Vestergaard C, Bilsborough J, Olsen UB, Grønhoj-Larsen C, et al. Anti-interleukin-31-antibodies ameliorate scratching behaviour in NC/Nga mice: a model of atopic dermatitis. *Exp Dermatol* 2009;18:35-43.
23. Hawro T, Saluja R, Weller K, Altrichter S, Metz M, Maurer M. Interleukin-31 does not induce immediate itch in atopic dermatitis patients and healthy controls after skin challenge. *Allergy* 2014;69:113-7.
24. Kasutani K, Fujii E, Ohyama S, Adachi H, Hasegawa M, Kitamura H, et al. Anti-IL-31 receptor antibody is shown to be a potential therapeutic option for treating itch and dermatitis in mice. *Br J Pharmacol* 2014;171:5049-58.
25. Nemoto O, Shiramoto M, Hanada R, Matsuki S, Imayama S, Kato M, et al. Safety and tolerability of a humanized monoclonal antibody to the Interleukin-31 receptor; results of a phase I, single ascending dose study, in healthy volunteers and patients with atopic dermatitis. Abstract presented at: European Academy of Dermatology and Venereology Meeting, Istanbul, Turkey; October 2-6, 2015.
26. Islam S, Kjällquist U, Moliner A, Zajac P, Fan JB, Lönnerberg P, et al. Highly multiplexed and strand-specific single-cell RNA 5' end sequencing. *Nat Protoc* 2012;7:813-28.
27. Bareyre FM, Garzorz N, Lang C, Misgeld T, Büning H, Kerschensteiner M. In vivo imaging reveals a phase-specific role of STAT3 during central and peripheral nervous system axon regeneration. *Proc Natl Acad Sci U S A* 2011;108:6282-7.
28. Stott B, Lavender P, Lehmann S, Pennino D, Durham S, Schmidt-Weber CB. Human IL-31 is induced by IL-4 and promotes TH2-driven inflammation. *J Allergy Clin Immunol* 2013;132:446-54.
29. Murota H, El-latif MA, Tamura T, Katayama I. Olopatadine hydrochloride decreases tissue interleukin-31 levels in an atopic dermatitis mouse model. *Acta Derm Venereol* 2014;94:78-9.
30. Slaets H, Nelissen S, Janssens K, Vidal PM, Lemmens E, Stinissen P, et al. Oncostatin M reduces lesion size and promotes functional recovery and neurite outgrowth after spinal cord injury. *Mol Neurobiol* 2014;50:1142-51.
31. Murphy M, Reid K, Hilton DJ, Bartlett PF. Generation of sensory neurons is stimulated by leukemia inhibitory factor. *Proc Natl Acad Sci U S A* 1991;88:3498-501.
32. Moidunny S, Vinet J, Wesseling E, Bijzet J, Shieh CH, van Ijzendoorn SC, et al. Adenosine A2B receptor-mediated leukemia inhibitory factor release from astrocytes protects cortical neurons against excitotoxicity. *J Neuroinflammation* 2012;9:198.
33. Gallagher D, Gutierrez H, Gavalda N, O'Keeffe G, Hay R, Davies AM. Nuclear factor-kappaB activation via tyrosine phosphorylation of inhibitor kappaB-alpha is crucial for ciliary neurotrophic factor-promoted neurite growth from developing neurons. *J Neurosci* 2007;27:9664-9.
34. Liu H, Liu G, Bi Y. CNTF regulates neurite outgrowth and neuronal migration through JAK2/STAT3 and PI3K/Akt signaling pathways of DRG explants with gp120-induced neurotoxicity in vitro. *Neurosci Lett* 2014;569:110-5.
35. Gallo G, Letourneau PC. Regulation of growth cone actin filaments by guidance cues. *J Neurobiol* 2004;58:92-102.
36. Li Y, Jia YC, Cui K, Li N, Zheng ZY, Wang YZ, et al. Essential role of TRPC channels in the guidance of nerve growth cones by brain-derived neurotrophic factor. *Nature* 2005;434:894-8.
37. Dou YC, Hagströmer L, Emtestam L, Johansson O. Increased nerve growth factor and its receptors in atopic dermatitis: an immunohistochemical study. *Arch Dermatol Res* 2006;298:31-7.
38. Tominaga M, Ogawa H, Takamori K. Decreased production of semaphorin 3A in the lesional skin of atopic dermatitis. *Br J Dermatol* 2008;158:842-4.
39. Cosker KE, Segal RA. Neuronal signaling through endocytosis. *Cold Spring Harb Perspect Biol* 2014;6(2).
40. Patapoutian A, Reichardt LF. Trk receptors: mediators of neurotrophin action. *Curr Opin Neurobiol* 2001;11:272-80.
41. Christie KJ, Zochodne D. Peripheral axon regrowth: new molecular approaches. *Neuroscience* 2013;240:310-24.
42. Shimada T, Fournier AE, Yamagata K. Neuroprotective function of 14-3-3 proteins in neurodegeneration. *Biomed Res Int* 2013;2013:564534.
43. Saijilafu, Hur EM, Liu CM, Jiao Z, Xu WL, Zhou FQ. PI3K-GSK3 signalling regulates mammalian axon regeneration by inducing the expression of Smad1. *Nat Commun* 2013;4:2690.
44. Guo W, Jiang H, Gray V, Dedhar S, Rao Y. Role of the integrin-linked kinase (ILK) in determining neuronal polarity. *Dev Biol* 2007;306:457-68.
45. Quarta S, Baeumer BE, Scherbakov N, Andratsch M, Rose-John S, Dechant G, et al. Peripheral nerve regeneration and NGF-dependent neurite outgrowth of adult sensory neurons converge on STAT3 phosphorylation downstream of neurotrophic cytokine receptor gp130. *J Neurosci* 2014;34:13222-33.
46. Selvaraj BT, Frank N, Bender FL, Asan E, Sendtner M. Local axonal function of STAT3 rescues axon degeneration in the pmn model of motoneuron disease. *J Cell Biol* 2012;199:437-51.
47. Goswami C, Rademacher N, Smalla KH, Kalscheuer V, Ropers HH, Gundelfinger ED, et al. TRPV1 acts as a synaptic protein and regulates vesicle recycling. *J Cell Sci* 2010;123:2045-57.

METHODS

Mice and sample collection

Six to 8-week-old wild-type C57BL/6 and *Trpv1* knockout mice were kept under specific pathogen-free conditions. *Il31*Tg mice specifically overexpressing *Il31* under the E μ -Lck promoter in lymphocytes^{E1} and control littermates were housed for up to 9 months under specific pathogen-free conditions until characteristic lesions developed spontaneously. Subsequently, punch biopsy specimens from lesional and nonlesional skin were collected. An IL-31 pump study in BALB/c mice was performed. Briefly, BALB/c mice received 20 mg/d recombinant mouse IL-31 (mIL-31; ZymoGenetics, Seattle, Wash) for 14 days delivered subcutaneously through a miniosmotic pump (Alzet Osmotic Pump; Durect, Cupertino, Calif). The skin phenotype was monitored daily and scored based on pruritus, hair loss, and lesion development: 0, no scratching or hair loss; 1, minimal scratching and thinning of the coat in small areas; 2, scratching with minor hair loss; 3, scratching with moderate hair loss and lesion development; and 4, excessive scratching with severe hair loss and lesion development. Skin biopsy specimens were taken from the area in which the pump was dispensing mIL-31. All animal procedures were approved by the ZymoGenetics Institutional Animal and Care and Use Committee or by the local government committee, the "Landesamt fuer Natur, Umwelt und Verbraucherschutz Nordrhein-Westfalen."

Preparation and treatment of DRG neurons

To prepare sensory neurons from dissociated DRG neurons, adult C57BL/6 mice were killed, and DRGs from the lumbar, thoracic, and cervical regions were removed. DRGs were trimmed of connective tissue and nerve roots and then treated with 3 mg/mL collagenase (Sigma-Aldrich, St Louis, Mo) and 0.25 mg/mL trypsin (PAA Laboratories/GE Healthcare) for 30 minutes. DRGs were triturated for dissociation to prepare a single-cell suspension. To generate whole DRG explants, DRGs derived from C57BL/6 mice or *Trpv1* knockout mice were isolated, as described above, except that connective tissue was digested with 0.3% collagenase for 30 minutes only. Both dissociated DRG neurons and whole DRG explants were plated onto cell-culture dishes (for RNA and protein extraction) or glass slides (for immunofluorescence) coated with poly-L-lysine (0.1–1 mg/mL, Sigma-Aldrich) and laminin (5 μ g/mL, Sigma-Aldrich). Cells were cultured in minimal essential medium supplemented with 10% horse serum, 1% penicillin/streptomycin, 1% vitamins, 1% N2-supplement, and 2% B27-supplement for recovery. Cultured DRGs were stimulated with 100 ng/mL mIL-31 (ZymoGenetics) or 10 ng/mL NGF (Sigma-Aldrich) for the indicated time points. In selected experiments 2 μ mol/L (dissociated DRG neurons) or 20 μ mol/L (whole DRG explants) of the STAT3 inhibitor V/Statitc (Calbiochem, San Diego, Calif) was applied 1 hour before IL-31 stimulation.

Immunofluorescence and image analysis

OCT-embedded skin samples were cut in 20- μ m-thick sections to analyze cutaneous innervation. Sections were either fixed with Zamboni's fixative (MORPHISTO, Frankfurt, Germany) or 4% paraformaldehyde, blocked with 2% BSA and 10% donkey serum in 0.5% Triton X-100 containing PBS, and stained with 2.5 μ g/mL rabbit anti-PGP9.5 pAb (EMD Millipore, Billerica, Mass), anti-rabbit Alexa Fluor 555 (Invitrogen), and 4'-6-diamidino-2-phenylindole dihydrochloride (DAPI; Molecular Probes, Eugene, Ore). Confocal image stacks at \times 20 magnification were taken with the Zeiss LSM 510 (Zeiss, Oberkochen, Germany) supplemented with Zen software and "flattened" into a single image before nerve fiber quantification. Cutaneous PGP9.5⁺ fibers were quantified in preprocessed images by 3 independent blind researchers. DRG neurons were first fixed with 1% paraformaldehyde/7.5% sucrose for 30 minutes and then for another 30 minutes in 2% paraformaldehyde/15% sucrose to quantify axonal growth and to identify the cellular IL-31RA localization. DRG neurons were stained with 10 μ g/mL anti- β III-tubulin (Sigma-Aldrich), 14.8 μ g/mL rat anti-mouse IL-31RA mAb (ZymoGenetics), and anti-rabbit Alexa Fluor 488 or anti-rat Alexa Fluor 594 (both Invitrogen), according to standard methods. Images were taken with a Zeiss Cell Observer, Axiovision and

Mosaik software, or a Zeiss LSM 510 supplemented with Zen software (all from Zeiss). The length of each neurite was measured as the distance from the end of the neurite straight back to the DRG body radially.^{E2} Cryopreserved, OCT-embedded whole DRGs plucked from the spinal columns of C57BL/6 mice were cut in 10- μ m-thick sections. Sections were stained with 14.8 μ g/mL rat anti-mouse IL-31RA (ZymoGenetics), 2.9 μ g/mL rabbit anti-mouse TrkA (Abcam, Cambridge, United Kingdom), anti-rat Alexa Fluor 555, and anti-rabbit Alexa Fluor 488 (both from Invitrogen), according to standard methods, to visualize the distribution of IL-31- and NGF-responsive neurons. Photographs were taken with the Zeiss Cell Observer. For all immunofluorescence staining, at least 3 independent experiments were performed.

RNA-Seq and data analysis

The STRT method was used,^{E3} with minor modifications, to measure transcription initiation at the 5' end of polyA⁺ transcripts starting from 10 ng of total RNA as template. RNA samples from DRG neurons (from n = 3 independent experiments) were arranged in the plate, and each one was sequenced with an individual barcode. The capture buffer contained 10 mmol/L Tris-HCl (pH 8.0), 0.1% Triton X-100, 800 nmol/L T30-VN-oligo, 2 mmol/L dNTP mixture, and 2 μ mol/L template switching oligos barcoding the sample. The cDNAs were pooled into one tube by using 10% PEG-6000 and 0.9 mol/L NaCl and amplified by using 14 cycles of PCR and 10 additional cycles to introduce the complete sets of adapters for Illumina sequencing (Illumina, San Diego, Calif). The libraries were size selected (200–400 bp) by using sequential AMPure XP bead selection protocol and 0.7 \times and 0.22 \times ratios.

The sequences of the STRT libraries were preprocessed to (1) demultiplex by sample barcodes; (2) exclude redundant reads to reduce PCR bias by unique molecular identifiers^{E4}; (3) align the reads to the mouse reference genome mm9, the mouse ribosomal DNA repeating unit (GenBank: BK000964), and spike-in sequences by using TopHat^{E5}; (4) quantify the expression levels in 50-bp strand-specific windows sliding in 25-bp steps; and (5) perform the basal quality check of the library and the sequencing. Then the differential expression was tested by using SAMstr.^{E6}

For analysis, only sequences that aligned to coding DNA sequence, coding upstream, and coding 5' untranslated region were selected, and duplicates were removed. Annotation was done manually with information in GenBank, PubMed, and pfam alignments to assign individual genes to functional classes to generate a detailed (level 1: 44 classes for IL-31-cultured DRG neurons and 48 classes for NGF cultured DRG neurons) annotation or an overview (level 2: 10 classes for both culture conditions) with broader functional classes. Genes that were not characterized and did not have any informative pfam motifs were annotated as "Unknown." Summary (level 2) data sets were then plotted in a bar chart format to compare functional classes after induction of gene expression by IL-31 or NGF.

Biological functions associated with differentially expressed genes were identified by using IPA. We performed a global canonical pathway enrichment analysis and functional enrichment analysis of diseases and functions. Three functional categories of interest were considered: cell death, cellular movement, and nervous system development. Differentially expressed genes associated with NGF and IL-31 were analyzed independently to identify biological functions and were ranked were based on the summed $-\log(P)$ value across both NGF and IL-31.

Western blotting

Proteins from IL-31-activated DRG neurons were harvested with Roti-Load buffer (Carl Roth) supplemented with 2-mercaptoethanol at the indicated time points and boiled for 10 minutes. Whole DRG lysates were separated by means of SDS-PAGE and transferred onto nitrocellulose membranes, according to standard methods. The primary antibodies anti-pERK1/2 (Thr202/Tyr204 [1:1000]) and anti-pSTAT3 (Tyr705 [1:2000]); both from Cell Signaling, Danvers, Mass) and 0.3 μ g/mL anti- β III-tubulin (Sigma-Aldrich) and appropriate peroxidase-conjugated secondary antibodies (GE Healthcare, Fairfield, Conn) were used, according to the manufacturer's

instructions. Changes in phosphorylation status were evaluated by using ImageJ software (National Institutes of Health, Bethesda, Md).

Quantitative real-time PCR

RNA was prepared from IL-31- and NGF-activated DRG neurons with the RNeasy kit (Qiagen) and reverse transcribed with SuperScript II (Invitrogen), according to the manufacturer's instructions. Quantitation of mRNA levels was performed by using real-time fluorescence detection with Absolute SYBR Green ROX mix (Applied Biosystems, Foster City, Calif). The primers used were as follows: *Il31ra* forward, 5'-tcaagacattgtcaatcagtgtg-3'; *Il31ra* reverse, 5'-gtcactgtttgatgctaagtagaaga-3'; *Shroom3* forward, 5'-ggggcttcaccctgaaag-3'; *Shroom3* reverse, 5'-ttgcccccttctcaatct-3'; *Nts* forward, 5'-agctggtgtgcctgactctc-3'; *Nts* reverse, 5'-ccagggtctcacatcttct-3'; *Rcan1* forward, 5'-ggctgca-caagaccgagt-3'; *Rcan1* reverse, 5'-tgtgaactctatgtgtaagctga-3'; *Sema6d* forward, 5'-tttgccttccataaccacagc-3'; *Sema6d* reverse, 5'-ctggactcccaccgtacac-3'; *Cyth2* forward, 5'-tctcaaccagaccgagag-3'; *Cyth2* reverse, 5'-gccgctccaagtcttcac-3'; *Prph* forward, 5'-tctgatcaggacaattgagacc-3'; and *Prph* reverse, 5'-cactgtgctgttctctctgg-3'. Primers and probes specific for 18S RNA were obtained from Life Technologies (Darmstadt, Germany). Target gene

expression was analyzed on an Applied Biosystems Prism 7000 supplemented with SDS 1.2.3 software, and the expression profile was normalized by using 18S expression.

REFERENCES

- E1. Dillon SR, Sprecher C, Hammond A, Bilsborough J, Rosenfeld-Franklin M, Pre-snell SR, et al. Interleukin 31, a cytokine produced by activated T cells, induces dermatitis in mice. *Nat Immunol* 2004;5:752-60.
- E2. Deister C, Schmidt CE. Optimizing neurotrophic factor combinations for neurite outgrowth. *J Neural Eng* 2006;3:172-9.
- E3. Islam S, Kjällquist U, Moliner A, Zajac P, Fan JB, Lönnerberg P, et al. Highly multiplexed and strand-specific single-cell RNA 5' end sequencing. *Nat Protoc* 2012;7:813-28.
- E4. Kivioja T, Vähärautio A, Karlsson K, Bonke M, Enge M, Linnarsson S, et al. Counting absolute numbers of molecules using unique molecular identifiers. *Nat Methods* 2011;9:72-4.
- E5. Trapnell C, Pachter L, Salzberg SL. TopHat: discovering splice junctions with RNA-Seq. *Bioinformatics* 2009;25:1105-11.
- E6. Bareyre FM, Garzorz N, Lang C, Misgeld T, Büning H, Kerschensteiner M. In vivo imaging reveals a phase-specific role of STAT3 during central and peripheral nervous system axon regeneration. *Proc Natl Acad Sci U S A* 2011;108:6282-7.

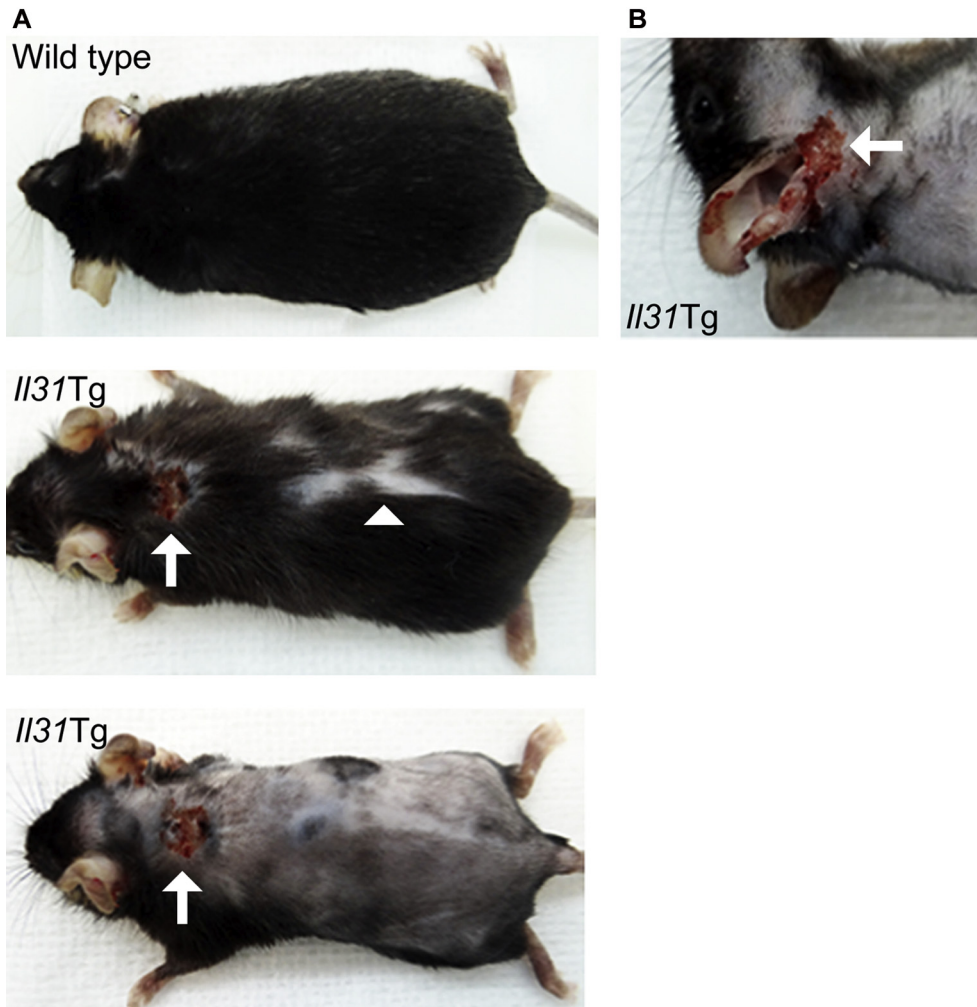


FIG E1. Skin phenotype in *I31Tg* mice. Spontaneous development of skin lesions in *I31Tg* mice in the nape of the neck (*white arrow*, **A**) and ears (**B**), as well as development of signs of hair loss on the back (*white arrowhead*).

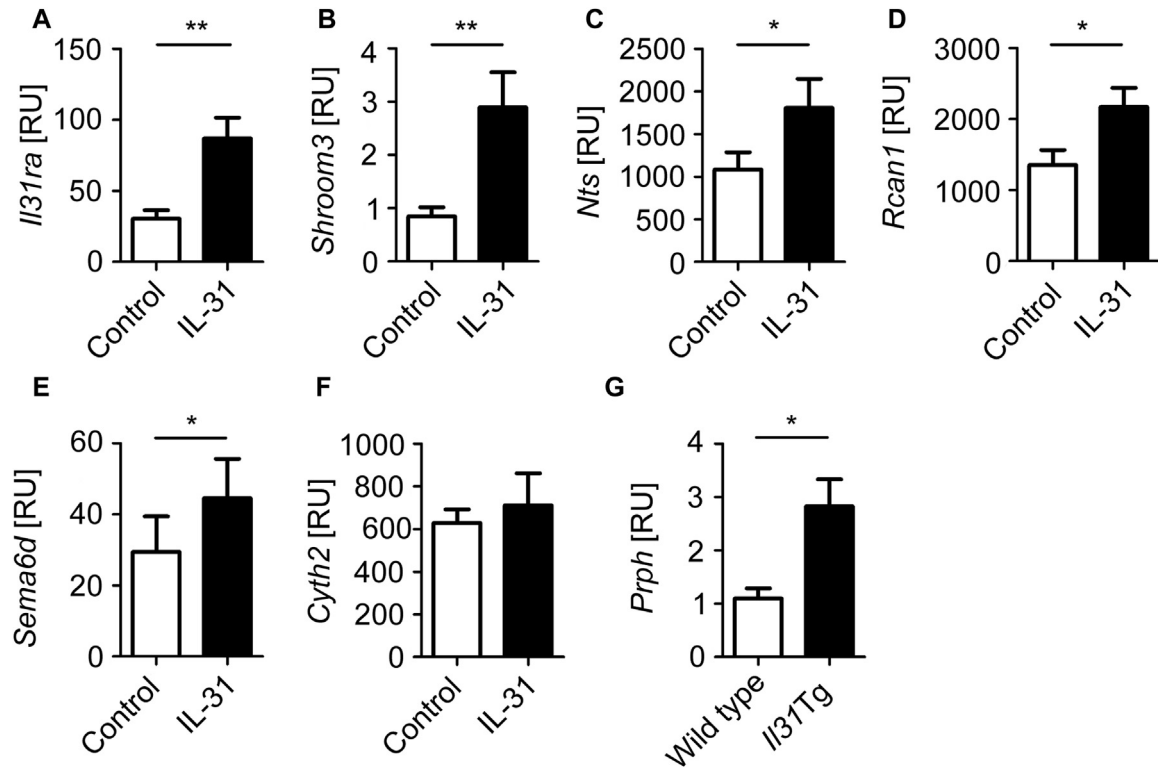


FIG E2. Validation of RNA-Seq data *in vitro* and *ex vivo*. **A-F**, Validation of 6 randomly selected genes in biological replicates of mIL-31-activated DRG neurons. **G**, Expression profile of the neuron-specific gene *Prph* in healthy skin from C57BL/6 mice and *Il31Tg* mice. * $P < .05$ and ** $P < .01$.

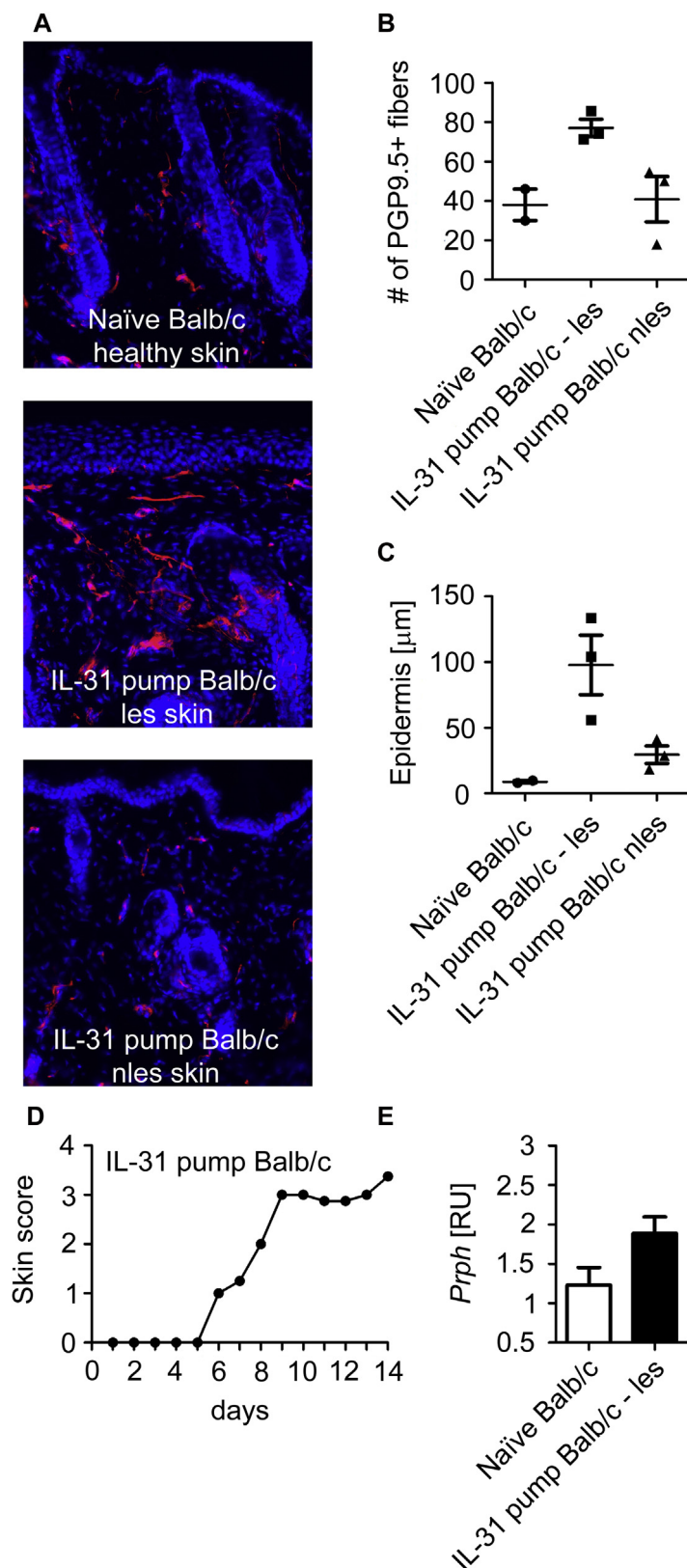


FIG E3. Pump-delivered mIL-31 promotes nerve fiber elongation, pruritus, and epidermal thickening in BALB/c mice. **A-C**, Analysis of PGP9.5⁺ nerve fibers and epidermal thickening in BALB/c mice after continuous delivery of mIL-31 (14 days). **D**, Evaluation of pruritus and hair loss scores in IL-31 pump-supplemented BALB/c mice (score: 0, no scratching, animal appeared normal; 1, thinning of coat in small areas/scratching noted; 2, minor hair loss/scratching; 3, moderate hair loss/scratching; and 4, severe hair loss/excessive scratching). **E**, Quantitation of *Prph* expression in mIL-31 pump-treated mice.

Pathway enrichment

Canonical Pathway	NGF (-log(pval))	IL31 (-log(pval))
EIF2 Signaling	4,076162032	5,770226787
Oxidative Phosphorylation	2,373652826	3,561817896
Gluconeogenesis I	2,75247761	2,538198233
Mitochondrial Dysfunction	2,18297669	3,066744457
14-3-3-mediated Signaling	0,977161324	4,18874801
Regulation of eIF4 and p70S6K Signaling	0,771230656	4,290506996
mTOR Signaling	0,559983575	4,161762165
Unfolded protein response	1,808776853	2,457844517
Glycolysis I	2,75247761	1,475661409
ERK5 Signaling	0,903754489	3,096407492
Cell Cycle: G2/M DNA Damage Checkpoint Regulation	1,086662778	2,612326854
Huntingtons Disease Signaling	1,131338349	2,268249295
ERK/MAPK Signaling	1,444333791	1,663914012
p70S6K Signaling	0,49296076	2,584065887
Androgen Signaling	1,028634218	2,028639509
Corticotropin Releasing Hormone Signaling	1,637297387	1,399660473
Lipid Antigen Presentation by CD1	1,582793893	1,444153866
Cholesterol Biosynthesis I	2,166794329	0,853384957
Cholesterol Biosynthesis II (via 24,25-dihydrolanosterol)	2,166794329	0,853384957
NAD Phosphorylation and Dephosphorylation	2,166794329	0,853384957
Cholesterol Biosynthesis III (via Desmosterol)	2,166794329	0,853384957
PI3K/AKT Signaling	0,474183421	2,512556553
p38 MAPK Signaling	1,563830177	1,329732885
IGF-1 Signaling	0,615321847	2,271162156
ILK Signaling	0,967964816	1,674021323
Glioma Invasiveness Signaling	1,746168958	0,852280425
Glutamate Receptor Signaling	1,746168958	0,852280425
cAMP-mediated signaling	2,248397132	0,33258727
NRF2-mediated Oxidative Stress Response	2,078200976	0,462608915
Protein Kinase A Signaling	1,081369893	1,445574343
Myc Mediated Apoptosis Signaling	0,962883602	1,530998754
Germ Cell-Sertoli Cell Junction Signaling	0,336079235	1,966388416
Ephrin B Signaling	0,292521918	1,994703268
Remodeling of Epithelial Adherens Junctions	0,850144967	1,356374596
tRNA Charging	2,19647265	
Breast Cancer Regulation by Stathmin1	0,547707608	1,624231874
Superpathway of Cholesterol Biosynthesis	1,522658161	0,556367364
Gli Signaling	1,528871761	0,393308768
Axonal Guidance Signaling	0	1,913094255
Coagulation System	1,344717051	0,47598352
Nitric Oxide Signaling in the Cardiovascular System	1,800409145	0
Antigen Presentation Pathway	1,301192155	0,456528928
Epoxysqualene Biosynthesis	1,714124955	
Neurotrophin/TRK Signaling	0,318527905	1,372379138
Asparagine Degradation I		1,63907355
Adenine and Adenosine Salvage I		1,63907355
Endoplasmic Reticulum Stress Pathway		1,617513148
PEDF Signaling	0,300852237	1,310056029
Diphthamide Biosynthesis	1,54013191	
Small Cell Lung Cancer Signaling	1,497881299	
NGF Signaling		1,449110891
PCP pathway		1,439462254
Creatine-phosphate Biosynthesis		1,343036327
eNOS Signaling	1,31226812	0

FIG E4. Data set 2: IPA output. Data are related to pathway enrichment and functional annotations. Data set 1: accession to RNA-Seq raw data; data are uploaded with the European Nucleotide Archive at <http://www.ebi.ac.uk/ena/data/view/PRJEB9128> and do not appear here.

Cell Death IL-31 Categories	Diseases or Functions Annotation	p-Value	Activation z-score	Molecules	#
Cell Death and Survival	necrosis	0,000117	-1,455	ADRM1,ALDOA,APRT,ATF3,ATF4,ATP1A1,AU RKA,BDNF,CCT5,CD274,CLU,CST3,CTBP1,D DIT3,DTYMK,FKBP4,GNAO1,GNB2,GSTM5,H SPA4,ILK,ITGA7,LDHA,LRPAP1,MAD2L1,MA PK3,NDEL1,NEFH,Nppb,NSMCE1,NTS,PAFA H2,PGRMC1,PIK3IP1,PLA2G7,PROCR,PSAP, PTTG1,Pvr,RABGGTA,RAN,RHOA,RPS3,RPS 6KB1,RTN4,SCYL1,SDC4,SERPINB2,SIN3B, SIVA1,SNCA,SPARC,SPIN1,THBD,TNIP2,TU BA1A,TUBB,TUBB3,VTI1B,XAF1,YWHAB,YW HAQ,YWHAZ	63
Cell Death and Survival	apoptosis of neurons	0,000182	-0,559	ATF3,ATF4,BDNF,DDIT3,GNAO1,GSTM5,ILK, LRPAP1,NDEL1,NTS,PLA2G7,RHOA,RPS3,SI VA1,SNCA,VTI1B,YWHAB	17
Cell Death and Survival	apoptosis of male germ cells	0,000307		BDNF,CLU,EHD1,HSPA4,HSPBP1,INSL6,PAF AH1B2	7
Cell Death and Survival	cell death of fibroblast cell lines	0,000418	0,928	ATF3,ATF4,CLU,DDIT3,FKBP4,GNB2,GSTM5, 16 ILK,MAPK3,NSMCE1,Pvr,RHOA,SDC4,SERPI NB2,SIVA1,YWHAZ	
Cell Death and Survival	cell death	0,000522	-1,796	ADRM1,ALDOA,APRT,ARL6IP5,ATF3,ATF4,A TP1A1,AURKA,BDNF,CANX,CCT5,CD274,CL U,CST3,CTBP1,CTSH,CYSLTR2,DDIT3,DTY MK,EHD1,FKBP4,GABARAP,GNAO1,GNB2,G STM5,HSPA4,HSPBP1,IL4R,ILK,INSL6,ITGA7 ,LDHA,LRPAP1,MAD2L1,MAL,MAPK3,NDEL1, NEFH,Nppb,NSMCE1,NTS,PAFAH1B2,PAFAH 2,PGRMC1,PIK3IP1,PLA2G7,PROCR,PSAP,P TTG1,Pvr,RABGGTA,RAN,RHOA,RPS3,RPS6 KB1,RTN4,SCYL1,SDC4,SERPINB2,SH3BGR L3,SIN3B,SIVA1,SNCA,SPARC,SPIN1,THBD, TNIP2,TUBA1A,TUBB,TUBB3,VTI1B,XAF1,Y WHAB,YWHAQ,YWHAZ	75
Cell Death and Survival	neuronal cell death	0,000612	-0,086	ATF3,ATF4,BDNF,CLU,DDIT3,GNAO1,GSTM5 22 ,ILK,LDHA,LRPAP1,NDEL1,NEFH,NTS,PIK3IP 1,PLA2G7,RHOA,RPS3,SIVA1,SNCA,VTI1B,Y WHAB,YWHAZ	
Cardiovascular System Development and Function, Cell Death and Survival	cell viability of endothelial cells	0,00064	1,951	BDNF,DDIT3,ILK,ITGB1BP1,TNIP2	5
Cell Death and Survival	cell death of connective tissue cells	0,00123	0,197	ATF3,ATF4,CLU,CTBP1,DDIT3,FKBP4,GNB2, 19 GSTM5,ILK,LRPAP1,MAPK3,NSMCE1,Pvr,RH OA,RPS6KB1,SDC4,SERPINB2,SIVA1,YWHA Z	
Cell Death and Survival	cell death of endothelial cells	0,00138	-1,706	ATF3,BDNF,DDIT3,MAPK3,Nppb,PROCR,RH 9 OA,THBD,TNIP2	
Cell Death and Survival	apoptosis	0,00142	-1,616	ALDOA,ARL6IP5,ATF3,ATF4,ATP1A1,AURKA, 60 BDNF,CANX,CD274,CLU,CST3,CTBP1,CTSH, DDIT3,DTYMK,EHD1,FKBP4,GABARAP,GNA O1,GNB2,GSTM5,HSPA4,HSPBP1,IL4R,ILK,I NSL6,ITGA7,LDHA,LRPAP1,MAD2L1,MAPK3, NDEL1,Nppb,NTS,PAFAH1B2,PAFAH2,PIK3IP 1,PLA2G7,PROCR,PSAP,PTTG1,RABGGTA,R HOA,RPS3,RPS6KB1,RTN4,SDC4,SH3BGR L3,SIN3B,SIVA1,SNCA,SPARC,THBD,TNIP2,T UBA1A,VTI1B,XAF1,YWHAB,YWHAQ,YWHA Z	
Cell Death and Survival, Cellular Compromise, Neurological Disease, Tissue Morphology	neurodegener ation of cholinergic neurons	0,00193		BDNF,SNCA	2
Cell Death and Survival	necrosis of epithelial tissue	0,00256	-0,476	ATF3,AURKA,BDNF,CLU,DDIT3,FKBP4,LDHA 18 ,MAPK3,NDEL1,Nppb,PROCR,RHOA,SIVA1,S NCA,SPARC,THBD,TNIP2,YWHAQ	

FIG E4. (Continued).

Cell Death and Survival, Cellular Compromise, Neurological Disease, Tissue Morphology	neurodegeneration of motor neurons	0,00257		BDNF,NEFH,SCYL1	3
Cell Death and Survival, Cellular Assembly and Organization, Cellular Development, Nervous System Development and Function, Tissue Development, Tissue Morphology	regeneration of axons	0,00263	0,068	BDNF,NDEL1,RHOA,RTN4	4
Cell Death and Survival	apoptosis of endothelial cells	0,00278	-1,446	ATF3,BDNF,DDIT3,MAPK3,Nppb,PROCR,RHOA,TNIP2	8
Cell Death and Survival	cell viability of breast cancer cell lines	0,00311	1,912	BDNF,CLU,EIF4A1,ILK,MAD2L1,PGRMC1,RHOA	7
Cell Death and Survival	cell death of hippocampal neurons	0,0032	0,44	BDNF,DDIT3,LRPAP1,RPS3,SNCA	5
Cell Death and Survival, Cellular Compromise, Neurological Disease, Tissue Morphology	neurodegeneration of neurites	0,0032	-0,747	LRPAP1,NEFH,PSAP,SCYL1,SNCA	5
Cell Death and Survival	apoptosis of kidney cells	0,00354	1,992	ATF3,ATP1A1,CLU,DDIT3,ILK	5
Cell Death and Survival	apoptosis of central nervous system cells	0,00416	-1,391	BDNF,GNAO1,LRPAP1,RHOA,RPS3,RPS6KB1,YWHAB	7
Cell Death and Survival	necrosis of kidney	0,00458	-0,184	APRT,ATF3,ATP1A1,CLU,DDIT3,GNB2,GSTM5,ILK,LDHA,NDEL1,SNCA,YWHAQ	12
Cell Death and Survival	cell death of tumor cell lines	0,00508	-0,763	ADRM1,ATF3,ATF4,ATP1A1,AURKA,BDNF,CT5,CD274,CLU,CTBP1,DDIT3,DTYMK,GNAO1,HSPA4,ILK,MAD2L1,MAPK3,PAFAH2,PGRMC1,PLA2G7,PSAP,PTTG1,RABGGTA,RHOA,RPS3,RPS6KB1,RTN4,SIN3B,SIVA1,SNCA,SPARC,SPIN1,TUBA1A,TUBB3,XAF1,YWHAZ	36
Cell Death and Survival	cell death of central nervous system cells	0,0061	-0,26	BDNF,CLU,DDIT3,GNAO1,LRPAP1,RHOA,RPS3,RPS6KB1,SNCA,YWHAB	10
Cell Death and Survival	cell death of retinal ganglion cells	0,00642		BDNF,LRPAP1,RHOA	3
Cell Death and Survival	apoptosis of tumor cell lines	0,00744	-1,535	ATF3,ATF4,AURKA,BDNF,CD274,CLU,CTBP1,DDIT3,DTYMK,HSPA4,ILK,MAD2L1,MAPK3,PAFAH2,PLA2G7,PSAP,PTTG1,RABGGTA,RHOA,RPS3,RPS6KB1,RTN4,SIN3B,SIVA1,SNCA,SPARC,TUBA1A,XAF1,YWHAZ	29
Cell Death and Survival	cell death of kidney cells	0,00865	0,252	ATF3,ATP1A1,CLU,DDIT3,GNB2,GSTM5,ILK,LDHA,NDEL1,SNCA,YWHAQ	11
Cell Death and Survival	apoptosis of cerebral cortex cells	0,00869	-1,479	BDNF,GNAO1,LRPAP1,RPS3,YWHAB	5
Cell Death and Survival	cell death of cytotoxic T cells	0,00952		CD274,CST3	2
Cell Death and Survival	cell death of neuroblastoma cell lines	0,00968	-0,546	BDNF,CCT5,CLU,DDIT3,GNAO1,SNCA,TUBA1A	7
Cell Death and Survival	regeneration of cells	0,00971	0,468	BDNF,DDIT3,NDEL1,RHOA,RTN4	5
Cell Death and Survival	cell death of cerebral cortex cells	0,00978	-0,118	BDNF,CLU,DDIT3,GNAO1,LRPAP1,RPS3,SNCA,YWHAB	8
Cell Death and Survival	apoptosis of myeloma cell lines	0,0111	-1	ATF4,AURKA,DDIT3,RPS6KB1	4
Cancer, Cell Death and Survival, Tumor Morphology	apoptosis of TM4t cells	0,0115		DDIT3	1

FIG E4. (Continued).

Cell Death and Survival	apoptosis of antigen-specific T cells	0,0115		CD274	1
Cell Death and Survival	apoptosis of sperm	0,0115		BDNF	1
Cell Death and Survival, Cell Morphology, Cellular Function and Maintenance	autophagic cell death of pancreatic cancer cell lines	0,0115		AURKA	1
Cell Death and Survival	caspase-independent cell death of pancreatic cancer cell lines	0,0115		AURKA	1
Cell Death and Survival, Free Radical Scavenging	cytotoxicity of superoxide	0,0115		CLU	1
Cell Death and Survival, Connective Tissue Disorders, Developmental Disorder, Hematological Disease, Hereditary Disorder	hnsa due to aldolase a deficiency	0,0115		ALDOA	1
Cell Death NGF Categories	Diseases or Functions Annotation	p-Value	Activation z-score	Molecules	#
Cell Death and Survival	cell death	0,000000051	-3,681	AARS,AGA,AKAP12,ALDOA,ARIH2,BCR,BDNF,BHLHE40,CANX,CAV1,Ccl2,CCT7,DAXX,DNAJA1,DNAJC15,DUSP6,EEF1A1,EEF1E1,EIF3G,ELMO1,ERCC1,FKBP8,FSTL1,FTH1,GAL,GAS6,GLTSCR2,GSTM5,HES1,HIGD2A,HLA-E,HNRNPK,HSPH1,ID1,ID2,IFRD1,INHBA,IRAK4,LMNA,MYC,NCL,NUDCD3,PLAUR,PLK2,PRKAR1A,PRKG2,PROCR,PTGIR,PTGS2,RABGGTB,RND3,RNPS1,RPL10,RTN1,S1PR3,SCYL1,SERPINB2,SF3A1,SLC20A1,SMARCA2,SNCG,STAR,STX7,SYF2,THBD,TIMP1,TMCC3,TMEM173,TNC,TNFAIP8,TRIM10,TUBA1A,UBE2K,VAMP3,VIM,VPS33A,YWHAQ,ZNF274	78
Cell Death and Survival	necrosis of muscle	0,000000132	-1,735	ALDOA,CAV1,Ccl2,DAXX,DUSP6,EEF1A1,FS TL1,GAS6,ID1,ID2,INHBA,IRAK4,LMNA,MYC,NCL,SCYL1,THBD,TIMP1	18
Cell Death and Survival	cell death of muscle cells	0,000000474	-1,552	ALDOA,CAV1,DAXX,DUSP6,EEF1A1,FSTL1,GAS6,ID1,ID2,INHBA,IRAK4,LMNA,MYC,NCL,SCYL1,THBD,TIMP1	17
Cell Death and Survival	necrosis	0,00000126	-3,741	AARS,AGA,AKAP12,ALDOA,BCR,BDNF,BHLHE40,CAV1,Ccl2,CCT7,DAXX,DNAJC15,DUSP6,EEF1A1,EIF3G,ERCC1,FKBP8,FSTL1,FTH1,GAL,GAS6,GSTM5,HES1,HNRNPK,HSPH1,ID1,ID2,IFRD1,INHBA,IRAK4,LMNA,MYC,NCL,NUDCD3,PLAUR,PLK2,PRKAR1A,PROCR,PTGS2,RABGGTB,RND3,RPL10,RTN1,S1PR3,SCYL1,SERPINB2,SF3A1,SLC20A1,STAR,THBD,TIMP1,TMCC3,TMEM173,TNFAIP8,TRIM10,TUBA1A,UBE2K,VIM,VPS33A,YWHAQ,ZNF274	61
Cell Death and Survival	apoptosis	0,00000159	-3,586	AARS,AGA,AKAP12,ALDOA,ARIH2,BCR,BDNF,BHLHE40,CANX,CAV1,Ccl2,DAXX,DNAJA1,DNAJC15,DUSP6,EEF1A1,EEF1E1,ELMO1,ERCC1,FKBP8,FSTL1,FTH1,GAL,GAS6,GLTSCR2,GSTM5,HES1,HIGD2A,HNRNPK,HSPH1,ID1,ID2,INHBA,IRAK4,LMNA,MYC,NCL,PLAUR,PLK2,PRKAR1A,PROCR,PTGS2,RABGGTB,RND3,RNPS1,RPL10,RTN1,S1PR3,SLC20A1,SMARCA2,SNCG,STAR,SYF2,THBD,TIMP1,TNC,TNFAIP8,TRIM10,TUBA1A,VIM,YWHAQ,ZNF274	62

FIG E4. (Continued).

Cell Death and Survival	cell viability of tumor cell lines	0,0000608	2,57	ANKS1B,ATP5H,BDNF,BHLHE40,Calm1 (includes others),CAV1,DAXX,DUSP6,EEF2,EIF4A1,FT H1,GAS6,ID2,IRAK4,MYC,NPY1R,PLAUR,PL K2,PTGS2,RAD54B,SERPINB2,SF3A1,SMAR CA2,THBD,TNFAIP8	25
Cell Death and Survival	cell death of eye cells	0,0000903	-0,819	BDNF,GAS6,MYC,PLAUR,S1PR3,VAMP3,ZNF 274	7
Cell Death and Survival	cell death of retinal cells	0,0000472	-0,495	BDNF,GAS6,MYC,PLAUR,S1PR3,ZNF274	6
Cell Death and Survival	cell survival	0,0000771	3,17	ANKS1B,ATP5H,BCR,BDNF,BHLHE40,Brd4,C alm1 (includes others),CAV1,DAXX,DUSP6,EEF2,EIF4A1,ER CC1,FTH1,GAS6,HES1,ID2,IRAK4,LMNA,MY C,NPY1R,PLAUR,PLK2,PRKAR1A,PTGS2,RA D54B,S1PR3,SERPINB2,SF3A1,SMARCA2,T HBD,TIMP1,TNFAIP8,VIM,ZNF274	35
Cell Death and Survival	apoptosis of epithelial cells	0,000108	-0,759	DAXX,ERCC1,ID1,ID2,INHBA,MYC,NCL,PLA UR,PTGS2,RND3,SLC20A1,TIMP1	12
Cell Death and Survival	necrosis of epithelial tissue	0,000119	-1,361	BDNF,CAV1,DAXX,DUSP6,ERCC1,GAS6,ID1, ID2,INHBA,MYC,NCL,PLAUR,PROCR,PTGS2 ,RND3,SLC20A1,THBD,TIMP1,YWHAQ	19
Cell Death and Survival	apoptosis of prostate cancer cell lines	0,000125	-1,62	AKAP12,CAV1,ID1,INHBA,MYC,PLAUR,PRKA R1A,PTGS2,RABGGTB	9
Cell Death and Survival	cell death of tumor cell lines	0,00021	-2,865	AKAP12,BCR,BDNF,BHLHE40,CAV1,CCT7,D AXX,DNAJC15,EIF3G,FKBP8,FTH1,GAL,HES 1,HNRNPK,ID1,IFRD1,INHBA,LMNA,MYC,NC L,NUDCD3,PLAUR,PLK2,PRKAR1A,PTGS2,R ABGGTB,RTN1,S1PR3,SF3A1,TIMP1,TMCC3 ,TMEM173,TNFAIP8,TRIM10,TUBA1A,UBE2K	36
Cell Death and Survival, Gastrointestinal Disease, Hepatic System Disease	apoptosis of liver cells	0,000261	-0,388	DAXX,ERCC1,INHBA,MYC,NCL,PTGS2,SLC2 0A1,TIMP1	8
Cell Death and Survival	cell viability	0,000422	3,054	ANKS1B,ATP5H,BCR,BDNF,BHLHE40,Calm1 (includes others),CAV1,DAXX,DUSP6,EEF2,EIF4A1,ER CC1,FTH1,GAS6,ID2,IRAK4,LMNA,MYC,NPY 1R,PLAUR,PLK2,PRKAR1A,PTGS2,RAD54B, S1PR3,SERPINB2,SF3A1,SMARCA2,THBD,T IMP1,TNFAIP8	31
Cell Death and Survival, Gastrointestinal Disease, Hepatic System Disease	apoptosis of hepatocytes	0,00046	0	DAXX,ERCC1,INHBA,MYC,NCL,PTGS2,SLC2 0A1	7
Cell Death and Survival	apoptosis of muscle cells	0,000783	-1,925	ALDOA,DAXX,DUSP6,FSTL1,GAS6,ID2,INH B A,IRAK4,THBD,TIMP1	10
Cell Death and Survival	apoptosis of retinal cells	0,000862		BDNF,MYC,PLAUR,S1PR3	4
Cell Death and Survival	cell death of connective tissue cells	0,00111	-0,435	DAXX,EEF1A1,FKBP8,FTH1,GAS6,GSTM5,ID 17 1,ID2,LMNA,MYC,RPL10,SERPINB2,STAR,TI MP1,TNFAIP8,UBE2K,VIM	17
Cell Death and Survival	cell viability of breast cancer cell lines	0,00116	0,956	BDNF,BHLHE40,DAXX,EIF4A1,ID2,PTGS2,T NFAIP8	7
Cell Death and Survival	cell viability of melanoma cell lines	0,0013	1,165	DUSP6,GAS6,SMARCA2,TNFAIP8	4
Cell Death and Survival, Gastrointestinal Disease, Hepatic System Disease	necrosis of liver	0,00143	-1,058	AGA,DAXX,ERCC1,INHBA,MYC,NCL,PTGS2, SLC20A1,TIMP1	9
Cell Death and Survival	apoptosis of B-lymphocyte derived cell lines	0,0017	0,557	BCR,DAXX,FKBP8,HES1,INHBA,MYC	6
Cell Death and Survival	apoptosis of multilineage progenitor cells	0,00191		HES1,ID2	2

FIG E4. (Continued).

Cell Death and Survival	loss of exocrine cells	0,00191		CAV1,MYC	2
Cell Death and Survival	apoptosis of tumor cell lines	0,00239	-2,712	AKAP12,BCR,BDNF,BHLHE40,CAV1,DAXX,DNAJC15,FKBP8,FTH1,GAL,HES1,HNRNP1,INHBA,MYC,NCL,PLAUR,PLK2,PRKAR1A,PTGS2,RABGGTB,RTN1,S1PR3,TIMP1,TNFAIP8,TRIM10,TUBA1A	27
Cardiovascular System Development and Function, Cell Death and Survival	cell viability of endothelial cells	0,00274	1,972	BDNF,GAS6,PTGS2,S1PR3	4
Cell Death and Survival	cell death of heart cells	0,00314	-2,057	DAXX,FSTL1,INHBA,IRAK4,NCL,STAR,THBD,TIMP1	8
Cell Death and Survival	apoptosis of leukocyte cell lines	0,00318	-0,059	BCR,Ccl2,DAXX,FKBP8,HES1,INHBA,MYC	7
Cell Death and Survival, Gastrointestinal Disease, Hepatic System Disease	apoptosis of liver cell lines	0,00331		MYC,PTGS2,TIMP1	3
Cell Death and Survival	cell death of neuroblastoma cell lines	0,00385	-0,535	BDNF,CCT7,FKBP8,GAL,RTN1,TUBA1A,UBE2K	7
Cardiovascular System Development and Function, Cell Death and Survival	survival of vascular endothelial cells	0,00396		GAS6,PTGS2,S1PR3	3
Cell Death and Survival	apoptosis of RPE cells	0,00401		MYC,PLAUR	2
Cancer, Cell Death and Survival, Tumor Morphology	cell death of tumor cells	0,00426	1,601	BDNF,CAV1,DAXX,HES1,INHBA,MYC,PLAUR,PROCR,PTGS2,RND3,TIMP1	11
Cell Death and Survival	anoikis	0,0044	0,333	CAV1,EEF1A1,PLAUR,PTGS2,TIMP1	5
Cell Death and Survival	cell death of fibroblast cell lines	0,00534	0,314	DAXX,EEF1A1,FKBP8,FTH1,GAS6,GSTM5,ID1,ID2,MYC,RPL10,SERPINB2,VIM	12
Cell Death and Survival	cell death of muscle cell lines	0,00556		CAV1,EEF1A1,LMNA,MYC	4
Cell Death and Survival, Connective Tissue Development and Function	cell viability of fibroblast cell lines	0,0057	0,376	GAS6,LMNA,MYC,PRKAR1A,S1PR3	5
Cell Death and Survival	neuronal cell death	0,00574	-0,977	AARS,AGA,BDNF,Ccl2,DAXX,DUSP6,GAL,GAS6,GSTM5,HSPH1,ID2,INHBA,PTGS2,STAR,UBE2K,VPS33A,ZNF274	17
Cell Death and Survival	cell death of photoreceptors	0,00591		BDNF,GAS6,S1PR3	3
Cell Death and Survival, Cellular Compromise	fragmentation of nucleus	0,00636		INHBA,MYC,STAR	3
Cardiovascular Disease, Cell Death and Survival, Connective Tissue Disorders, Hematological Disease, Organismal Injury and Abnormalities, Renal and Urological Disease	hemolytic uremic syndrome	0,00681		PTGIR,THBD	2
Cell Death and Survival	susceptibility to excitotoxicity of neurons	0,00683		Ccl2,GAL,PTGS2	3
Cell Death and Survival	cell death of endothelial cells	0,00699	-0,973	BDNF,CAV1,DUSP6,GAS6,MYC,PROCR,THBD	7
Cell Death and Survival	cell death of nervous tissue cell lines	0,00701	0,187	DUSP6,GAS6,ID1,ID2	4
Cell Death and Survival	cell death of epithelial cells	0,0071	-0,603	DAXX,ERCC1,ID1,ID2,INHBA,MYC,NCL,PLAUR,PTGS2,RND3,SLC20A1,TIMP1,YWHAQ	13
Cellular Movement IL-31 Categories	Diseases or Functions Annotation	p-Value	Activation z-score	# Molecules	

FIG E4. (Continued).

Cellular Movement	cell movement of growth cone	0,000149		3
Cellular Movement, Skeletal and Muscular System Development and Function	migration of muscle cells	0,0000478	1,982	10
Cellular Movement	cell movement	0,000098	2,792	54
Cellular Movement	migration of cells	0,000173	2,926	49
Cellular Movement, Connective Tissue Development and Function	migration of fibroblast cell lines	0,000195	0,956	8
Cellular Movement, Connective Tissue Development and Function	cell movement of fibroblast cell lines	0,000223	1,715	9
Cardiovascular System Development and Function, Cellular Movement	migration of endothelial cells	0,000526	1,894	13
Cellular Movement, Skeletal and Muscular System Development and Function	migration of smooth muscle cells	0,000532	1,982	8
Cellular Movement	invasion of prostate cancer cell lines	0,000776	0,728	6
Cellular Movement	migration of lung cancer cells	0,00355		2
Cellular Movement, Connective Tissue Development and Function	scattering of fibroblast cell lines	0,00355		2
Cellular Movement	migration of brain cells	0,00491	1,965	5
Cell Morphology, Cellular Movement, Nervous System Development and Function	innervation of outer hair cells	0,00682		2
Cellular Movement, Embryonic Development	migration of mesenchymal cells	0,00682		2
Cellular Movement, Skeletal and Muscular System Development and Function	migration of vascular smooth muscle cells	0,00806		5
Cellular Movement	migration of connective tissue cells	0,00808	0,98	7
Cellular Movement	cell movement of connective tissue cells	0,00854	1,291	8
Cancer, Cellular Movement	invasion of endothelial cells	0,00884		3
Cellular Movement, Skeletal and Muscular System Development and Function	migration of myoblasts	0,00952		2
Cellular Movement	cell movement of epithelial cells	0,0105	1,016	6
Cellular Movement, Nervous System Development and Function	migration of cerebellar granule cell	0,011		2
Cellular Movement, Nervous System Development and Function	chemokinesis of granule cells	0,0115		1
Cellular Movement, Hematological System Development and Function	chemokinesis of hematopoietic cells	0,0115		1

FIG E4. (Continued).

Cellular Assembly and Organization, Cellular Function and Maintenance, Cellular Movement	dispersion of Golgi apparatus	0,0115		1	
Cellular Assembly and Organization, Cellular Function and Maintenance, Cellular Movement	dispersion of lysosome	0,0115		1	
Cellular Movement NGF Categories					
	Diseases or Functions Annotation	p-Value	Activation z-score	Molecules	#
Cardiovascular System Development and Function, Cellular Movement	migration of endothelial cells	0,00000516	1,95	BCAS3,BDNF,CAV1,GAS6,ID1,MYC,NCL,PLAUR,PTGS2,S1PR3,SCG2,SPRY4,THBD,TIMP1,VIM	15
Cellular Movement	cell movement	0,0000259	3,147	AKAP12,ALDOA,AP2M1,BCAS3,BCR,BDNF,BHLHE40,CAV1,Ccl2,DAXX,DCLK1,DNAJA1,DUSP6,ELMO1,FSTL1,FTH1,GAS6,HARS,HNRNPK,ID1,ID2,INADL,INHBA,IRAK4,LMNA,MYC,NCL,PLAUR,PRKAR1A,PROCR,PTGIR,PTGS2,RND3,RNH1,RPL13A,S1PR3,SCG2,SERPINB2,SNCG,SPRY4,THBD,TIMP1,TNC,TNF AIP6,TNFAIP8,Tpm1,TUBA1A,VDAC3,VIM	49
Cellular Movement, Reproductive System Development and Function	migration of gonadal cell lines	0,0000729	2,183	ELMO1,NCL,PLAUR,S1PR3,THBD	5
Cellular Movement	migration of cells	0,0000748	3,444	ALDOA,AP2M1,BCAS3,BCR,BDNF,BHLHE40,CAV1,Ccl2,DCLK1,ELMO1,FSTL1,FTH1,GAS6,HARS,HNRNPK,ID1,ID2,INADL,INHBA,IRAK4,LMNA,MYC,NCL,PLAUR,PRKAR1A,PROCR,PTGIR,PTGS2,RND3,RNH1,RPL13A,S1PR3,SCG2,SERPINB2,SNCG,SPRY4,THBD,TIMP1,TNC,TNFAIP6,TNFAIP8,Tpm1,TUBA1A,VIM	44
Cardiovascular System Development and Function, Cellular Movement	migration of vascular endothelial cells	0,000294	1,224	GAS6,ID1,NCL,PTGS2,S1PR3,SPRY4,THBD,TIMP1	8
Cellular Movement	cell movement of neuroglia	0,000456	-0,927	BCR,BDNF,CAV1,Ccl2,GAS6,TNC	6
Cellular Movement	homing	0,000698	0,913	AKAP12,BCR,BDNF,CAV1,Ccl2,DUSP6,GAS6,HARS,INHBA,IRAK4,MYC,PLAUR,PTGS2,RPL13A,S1PR3,SCG2,THBD	17
Cardiovascular System Development and Function, Cellular Movement	chemotaxis of vascular endothelial cells	0,00105		GAS6,PTGS2,THBD	3
Cellular Movement	homing of cells	0,00134	1,05	AKAP12,BCR,BDNF,CAV1,Ccl2,DUSP6,GAS6,HARS,INHBA,MYC,PLAUR,PTGS2,RPL13A,S1PR3,SCG2,THBD	16
Cellular Movement	cell movement of RPE cells	0,00137		MYC,PLAUR	2
Cellular Growth and Proliferation, Cellular Movement, Hematological System Development and Function	cytostasis of B-lymphocyte derived cell lines	0,00191		BCR,DAXX	2
Cellular Movement	cell movement of tumor cell lines	0,0025	2,085	AKAP12,AP2M1,BCR,CAV1,Ccl2,ELMO1,GAS6,HNRNPK,ID1,MYC,NCL,PLAUR,PTGS2,S1PR3,SNCG,THBD,TIMP1,TNC,TNFAIP8,VIM	20
Cellular Movement	chemotaxis	0,00262	1,227	BCR,BDNF,CAV1,Ccl2,DUSP6,GAS6,HARS,INHBA,IRAK4,PLAUR,PTGS2,RPL13A,S1PR3,SCG2,THBD	15
Cellular Assembly and Organization, Cellular Function and Maintenance, Cellular Movement, Nervous System Development and Function	endocytosis of synaptic vesicles	0,00301		CANX,PACSIN1,SNCG	3
Cellular Movement	invasion of cells	0,00321	2,091	BCR,BDNF,BHLHE40,CAV1,ELMO1,FSTL1,ID1,ID2,INHBA,MYC,PLAUR,PTGS2,RND3,RNH1,S1PR3,SNCG,THBD,TIMP1,VIM,YWHAQ	20

FIG E4. (Continued).

Cellular Movement	invasion of fibroblast cell lines	0,00328		CAV1,ELMO1,FSTL1,RND3	4
Cellular Movement	migration of tumor cells	0,00388	1,633	BDNF,CAV1,PLAUR,PTGS2,SERPINB2,TIMP1,TNC,VIM	8
Cellular Movement, Hematological System Development and Function, Immune Cell Trafficking	mobilization of antigen presenting cells	0,00401		Ccl2,IRAK4	2
Cell-To-Cell Signaling and Interaction, Cellular Movement, Hematological System Development and Function	recruitment of hematopoietic cells	0,00401		BDNF,Ccl2	2
Cellular Assembly and Organization, Cellular Movement, Nervous System Development and Function	transport of synaptic vesicles	0,00432		CANX,PACSIN1,SNCG,STX7	4
Cellular Movement	invasion of breast cancer cell lines	0,00445	1,238	CAV1,ID1,ID2,MYC,PLAUR,PTGS2,SNCG,TIMP1	8
Cellular Movement	chemotaxis of cells	0,00475	1,392	BCR,BDNF,CAV1,Ccl2,DUSP6,GAS6,HARS,1NHBA,PLAUR,PTGS2,RPL13A,S1PR3,SCG2,THBD	14
Cellular Movement	migration of brain cancer cell lines	0,00511	1,973	ELMO1,GAS6,NCL,PLAUR,TNC	5
Cellular Movement, Nervous System Development and Function	migration of neuroglia	0,00583	-1,131	BCR,BDNF,Ccl2,TNC	4
Cellular Movement	migration of fibrosarcoma cell lines	0,00591		AP2M1,HNRNPK,PLAUR	3
Cellular Movement, Hematological System Development and Function, Immune Cell Trafficking, Inflammatory Response	cell movement of dendritic cells	0,00675	-0,064	Ccl2,HARS,IRAK4,S1PR3,SCG2,TIMP1	6
Cellular Movement, Nervous System Development and Function	migration of interneurons	0,00681		BDNF,PLAUR	2
Cellular Movement	migration of tumor cell lines	0,00713	2,806	AP2M1,CAV1,ELMO1,GAS6,HNRNPK,ID1,MYC,NCL,PLAUR,PTGS2,S1PR3,SNCG,TIMP1,TNC,TNFAIP8,VIM	16
Nervous Development IL-31 Categories					
	Diseases or Functions Annotation	p-Value	Activation z-score	Molecules	#
Nervous System Development and Function	regeneration of peripheral nerve	0,00000603		ATF3,BDNF,CLU	3
Nervous System Development and Function	abnormal morphology of sensory ganglion	0,000395		BDNF,VTI1B	2
Nervous System Development and Function	abnormal morphology of sensory nervous system	0,000784		BDNF,ETV1	2
Embryonic Development, Nervous System Development and Function, Organ Development, Organismal Development, Tissue Development	formation of molecular layer of cerebellum	0,000784		BDNF,SLC17A6	2
Cellular Assembly and Organization, Nervous System Development and Function	quantity of neurite branches	0,0013		BDNF,RHOA	2
Cell Morphology, Nervous System Development and Function	length of neurites	0,00147	-0,036	BDNF,GDI1,LRPAP1,NDEL1,RHOA	5
Nervous System Development and Function, Neurological Disease	degradation of myelin sheath	0,00193		PSAP,SERPING1	2
Cell Morphology, Cellular Assembly and Organization, Nervous System Development and Function	diameter of axons	0,00193		BDNF,NEFH	2

FIG E4. (Continued).

Nervous System Development and Function, Tissue Morphology	morphology of nervous tissue	0,00208		BDNF,CKB,ETV1,LRPAP1,MAL,NDEL1,NEFH,PSAP,RHOA,RPS6KB1,RTN4,SCYL1,SLC17A6,SNCA,TUBA1A	15
Cellular Growth and Proliferation, Nervous System Development and Function	inhibition of neurons	0,00227		BDNF,KIF5B,RTN4	3
Cellular Assembly and Organization, Cellular Function and Maintenance, Nervous System Development and Function	quantity of neurites	0,00247	1,117	BDNF,CANX,LRPAP1,NEFH,SNCA	5
Cellular Development, Cellular Growth and Proliferation, Nervous System Development and Function, Tissue Development	outgrowth of neurons	0,00252	0,08	BDNF,CLU,FKBP4,GNAO1,ILK,MAPK3,NDEL1,NEFH,PSAP,RHOA,RTN4,TUBA1A,VTI1B,YWHAZ	14
Cell Death and Survival, Cellular Assembly and Organization, Cellular Development, Nervous System Development and Function, Tissue Development, Tissue Morphology	regeneration of axons	0,00263	0,068	BDNF,NDEL1,RHOA,RTN4	4
Cell Morphology, Hair and Skin Development and Function, Nervous System Development and Function	innervation of skin	0,00268		BDNF,ITGA7	2
Cellular Development, Cellular Growth and Proliferation, Nervous System Development and Function, Tissue Development	proliferation of sensory neurons	0,00268		BDNF,CLU	2
Cell Morphology, Nervous System Development and Function, Tissue Morphology	morphology of neurons	0,00406		BDNF,CKB,LRPAP1,MAL,NDEL1,NEFH,PSAP,RHOA,RPS6KB1,RTN4,SCYL1,SLC17A6,SNCA,TUBA1A	14
Nervous System Development and Function	myelination of nerves	0,00445		BDNF,MAL,RTN4	3
Cellular Development, Nervous System Development and Function, Tissue Development	myelination of neurons	0,0049		BDNF,ILK,RTN4	3
Cell Morphology, Cellular Assembly and Organization, Nervous System Development and Function	elongation of neurites	0,00509	0,594	ATF3,ITGA7,NDEL1,RHOA	4
Cell Morphology, Cellular Assembly and Organization, Cellular Function and Maintenance, Nervous System Development and Function	extension of neurites	0,00531	1,128	ATF3,BDNF,CYTH2,ILK,LRPAP1,NDEL1,RTN4	7
Cellular Assembly and Organization, Cellular Function and Maintenance, Nervous System Development and Function, Tissue Development	organization of neurofilaments	0,00562		NDEL1,NEFH	2
Cellular Assembly and Organization, Nervous System Development and Function	size of neurites	0,00562		BDNF,NEFH	2
Cell Morphology, Cellular Assembly and Organization, Nervous System Development and Function	elongation of axons	0,00589		ITGA7,NDEL1,RHOA	3
Cell Morphology, Cellular Assembly and Organization, Cellular Development, Cellular Growth and Proliferation, Nervous System Development and Function, Tissue Development	outgrowth of neurites	0,00605	-0,117	BDNF,FKBP4,GNAO1,ILK,MAPK3,NDEL1,NEFH,PSAP,RHOA,RTN4,TUBA1A,VTI1B,YWHAZ	13
Nervous System Development and Function	abnormal morphology of inferior ganglion of vagus nerve	0,00682		BDNF,VTI1B	2
Nervous System Development and Function	abnormal morphology of ventral root	0,00682		ETV1,NEFH	2
Cell Morphology, Cellular Movement, Nervous System Development and Function	innervation of outer hair cells	0,00682		BDNF,PSAP	2
Cell Morphology, Nervous System Development and Function	length of axons	0,00812		BDNF,RHOA	2

FIG E4. (Continued).

Embryonic Development, Nervous System Development and Function, Organ Development, Organismal Development, Tissue Development	formation of hippocampus	0,00837		BDNF,CST3,NDEL1,RHOA,SNCA	5
Cell Morphology, Cellular Assembly and Organization, Cellular Development, Cellular Function and Maintenance, Nervous System Development and Function, Tissue Development	axonogenesis	0,00914	0,751	ATF3,BDNF,GDI1,ILK,NDEL1,NEFH,RHOA,RTN4	8
Nervous System Development and Function	abnormal morphology of petrosal ganglion	0,011		BDNF,VT11B	2
Nervous System Development and Function	abnormal morphology of small trigeminal ganglion	0,011		BDNF,VT11B	2
Cellular Development, Cellular Growth and Proliferation, Embryonic Development, Nervous System Development and Function, Organ Development, Organismal Development, Tissue Development	development of hippocampal neurons	0,011		BDNF,RHOA	2
Cellular Movement, Nervous System Development and Function	migration of cerebellar granule cell	0,011		BDNF,NDEL1	2
Nervous System Development and Function	myelination of sciatic nerve	0,011		BDNF,MAL	2
Cell-To-Cell Signaling and Interaction, Nervous System Development and Function	synaptic transmission of hippocampal neurons	0,011		BDNF,SNCA	2
Cell Morphology, Cellular Assembly and Organization, Cellular Development, Cellular Function and Maintenance, Nervous System Development and Function, Tissue Development	morphogenesis of neurites	0,0113	0,665	ATF3,BDNF,CLU,DTNBP1,EHD1,ILK,NDEL1,NEFH,PFN1,RHOA,RPS6KB1,RTN4	12
Nervous System Development and Function, Organ Morphology	abnormal morphology of Golgi tendon organ	0,0115		ETV1	1
Cell Morphology, Nervous System Development and Function, Tissue Morphology	abnormal morphology of adrenergic neurons	0,0115		BDNF	1
Nervous System Development and Function	abnormal morphology of pacinian corpuscle	0,0115		ETV1	1
Auditory and Vestibular System Development and Function, Cell Morphology, Nervous System Development and Function, Organ Morphology, Tissue Morphology	abnormal morphology of type I vestibular hair cells	0,0115		BDNF	1
Cell-To-Cell Signaling and Interaction, Nervous System Development and Function	action potential of dopaminergic neurons	0,0115		BDNF	1
Cell-To-Cell Signaling and Interaction, Nervous System Development and Function	activation of striatal neurons	0,0115		BDNF	1
Cell-To-Cell Signaling and Interaction, Nervous System Development and Function, Tissue Development	aggregation of Cajal-Retzius neurons	0,0115		BDNF	1

FIG E4. (Continued).

Cell-To-Cell Signaling and Interaction, Cellular Assembly and Organization, Nervous System Development and Function	binding of synaptic vesicles	0,0115		SNCA	1
Cellular Movement, Nervous System Development and Function	chemokinesis of granule cells	0,0115		BDNF	1
Behavior, Nervous System Development and Function	declarative memory	0,0115		BDNF	1
Cellular Assembly and Organization, Nervous System Development and Function	density of neurofilaments	0,0115		NEFH	1
Cellular Development, Nervous System Development and Function, Tissue Development	differentiation of noradrenergic neurons	0,0115		BDNF	1
Cellular Development, Nervous System Development and Function, Tissue Development	differentiation of striatonigral neurons	0,0115		BDNF	1
Cell-To-Cell Signaling and Interaction, Cellular Function and Maintenance, Nervous System Development and Function	discharge of granule cells	0,0115		BDNF	1
Cell Morphology, Cellular Assembly and Organization, Cellular Development, Cellular Function and Maintenance, Nervous System Development and Function, Tissue Development	formation of Lewy neurites	0,0115		SNCA	1
Embryonic Development, Nervous System Development and Function, Organ Development, Organismal Development, Tissue Development	formation of internal granular layer of cerebellum	0,0115		BDNF	1
Cellular Growth and Proliferation, Nervous System Development and Function	formation of nervous tissue cell lines	0,0115		BDNF	1
Nervous System Development and Function	function of sensory nerve	0,0115		GLA	1
Cellular Function and Maintenance, Nervous System Development and Function	function of serotonergic neurons	0,0115		BDNF	1
Cellular Function and Maintenance, Nervous System Development and Function	hyperfunction of dopaminergic neurons	0,0115		BDNF	1
Nervous Development NGF Categories					
	Diseases or Functions Annotation	p-Value	Activation z-score	Molecules	#
Nervous System Development and Function	morphology of central nervous system	0,0000191		AGA,AKAP12,BCR,BDNF,CAV1,DCLK1,FKBP 8,GAL,GM2A,HES1,ID1,ID2,MYC,NPY1R,PLAUR,SLC17A6,TUBA1A,UPP1,VIM	19
Nervous System Development and Function, Tissue Morphology	quantity of striatal neurons	0,0000486		BDNF,FTH1,INHBA	3
Nervous System Development and Function, Organ Morphology, Organismal Development	morphology of brain	0,0000621		AGA,AKAP12,BCR,BDNF,CAV1,DCLK1,FKBP 8,GAL,GM2A,HES1,ID1,ID2,NPY1R,PLAUR,SLC17A6,TUBA1A,UPP1	17
Nervous System Development and Function, Organ Morphology, Organismal Development	abnormal morphology of brain	0,000117		AGA,AKAP12,BCR,BDNF,CAV1,DCLK1,FKBP 8,GAL,GM2A,HES1,ID1,ID2,NPY1R,PLAUR,SLC17A6,UPP1	16
Cellular Development, Embryonic Development, Nervous System Development and Function, Organismal Development, Tissue Development	differentiation of neural precursor cells	0,000169		BDNF,HES1,ID1,ID2	4

FIG E4. (Continued).

Nervous System Development and Function	morphology of nervous system	0,000187		AGA,AKAP12,BCR,BDNF,CANX,CAV1,Ccl2,D 23 CLK1,FKBP8,GAL,GM2A,HES1,ID1,ID2,LMN A,MYC,NPY1R,PLAUR,SCYL1,SLC17A6,TUB A1A,UPP1,VIM
Cell Morphology, Cell-To-Cell Signaling and Interaction, Nervous System Development and Function, Tissue Development	plasticity of synapse	0,0002		BDNF,CACNB4,ERCC1,P2RX3,PLK2,STAR,T 7 NC
Nervous System Development and Function	abnormal morphology of sympathetic nervous system	0,000279		BDNF,NPY1R 2
Nervous System Development and Function, Organ Morphology, Organismal Development	abnormal morphology of subventricular zone	0,000397		FKBP8,HES1,ID1,NPY1R 4
Cellular Development, Cellular Growth and Proliferation, Nervous System Development and Function	proliferation of neuroglia	0,00048	0,896	BDNF,HES1,PRKAR1A,RND3,S1PR3,TNC,VI 7 M
Embryonic Development, Nervous System Development and Function, Organ Development, Organismal Development, Tissue Development	formation of molecular layer of cerebellum	0,000555		BDNF,SLC17A6 2
Cell-To-Cell Signaling and Interaction, Nervous System Development and Function	synaptic transmission of nervous tissue	0,00062	0,686	BDNF,GAL,P2RX3,SLC17A6,SNCG,VDAC3 6
Nervous System Development and Function	abnormal morphology of nervous system	0,000892		AGA,AKAP12,BCR,BDNF,CANX,CAV1,Ccl2,D 20 CLK1,FKBP8,GAL,GM2A,HES1,ID1,ID2,LMN A,NPY1R,PLAUR,SCYL1,SLC17A6,UPP1
Cell-To-Cell Signaling and Interaction, Nervous System Development and Function	long-term potentiation of hippocampus	0,000906	1,599	BDNF,GAL,HNRNPK,KCNA4,PLK2,PRKAR1A 6
Cell Morphology, Nervous System Development and Function	morphology of astrocytes	0,000939		BCR,CAV1,HES1,VIM 4
Nervous System Development and Function, Tissue Morphology	morphology of nervous tissue	0,00108		AGA,BDNF,CAV1,DCLK1,GM2A,HES1,LMNA, 14 MYC,NPY1R,PLAUR,SCYL1,SLC17A6,TUBA 1A,UPP1
Cell Morphology, Nervous System Development and Function	morphology of central nervous system cells	0,00125		BCR,BDNF,CAV1,GM2A,HES1,TUBA1A,VIM 7
Nervous System Development and Function	abnormal morphology of lumbar 4 dorsal root ganglia	0,00137		BDNF,GAL 2
Nervous System Development and Function	abnormal morphology of dorsal root ganglion	0,0015		BDNF,FKBP8,GAL,HES1 4
Cell Morphology, Nervous System Development and Function, Tissue Morphology	abnormal morphology of neurons	0,00185		AGA,BDNF,CAV1,DCLK1,GM2A,HES1,LMNA, 12 NPY1R,PLAUR,SCYL1,SLC17A6,UPP1
Cell-To-Cell Signaling and Interaction, Nervous System Development and Function	activation of spinal neuron	0,00191		BDNF,PTGS2 2
Cellular Development, Nervous System Development and Function, Tissue Development	differentiation of GABAergic neurons	0,00191		BDNF,HES1 2
Nervous System Development and Function, Tissue Morphology	quantity of neurons	0,00198	2,119	AGA,BDNF,DCLK1,FTH1,GAL,HES1,INHBA,P 10 LAUR,SCYL1,SNCG
Cell-To-Cell Signaling and Interaction, Nervous System Development and Function	synaptic transmission	0,00204	-0,173	BDNF,CACNB4,Ccl2,FSTL1,GAL,NPY1R,P2R 11 X3,PTGS2,SLC17A6,SNCG,VDAC3
Cell-To-Cell Signaling and Interaction, Nervous System Development and Function	synaptic transmission of cells	0,00212	1,103	BDNF,Ccl2,FSTL1,GAL,NPY1R,P2RX3,SLC17 9 A6,SNCG,VDAC3

FIG E4. (Continued).

Cell Morphology, Nervous System Development and Function, Tissue Morphology	morphology of neurons	0,00237		AGA,BDNF,CAV1,DCLK1,GM2A,HES1,LMNA, NPY1R,PLAUR,SCYL1,SLC17A6,TUBA1A,UPP1	13
Nervous System Development and Function, Organ Morphology, Organismal Development	abnormal morphology of forebrain	0,0027		CAV1,DCLK1,FKBP8,GM2A,HES1,ID2,SLC17A6,UPP1	8
Cellular Assembly and Organization, Cellular Function and Maintenance, Cellular Movement, Nervous System Development and Function	endocytosis of synaptic vesicles	0,00301		CANX,PACSIN1,SNCG	3
Nervous System Development and Function, Tissue Morphology	quantity of interneurons	0,00301		BDNF,DCLK1,PLAUR	3
Nervous System Development and Function, Organ Morphology, Organismal Development	abnormal morphology of cerebellum	0,00316		AGA,AKAP12,BCR,FKBP8,GM2A,UPP1	6
Cell Morphology, Nervous System Development and Function	abnormal morphology of astrocytes	0,00396		BCR,CAV1,HES1	3
Cell Morphology, Cellular Assembly and Organization, Cellular Development, Cellular Function and Maintenance, Nervous System Development and Function, Organ Morphology, Tissue Development	branching of hippocampal neurons	0,00401		BDNF,PACSIN1	2
Nervous System Development and Function, Organ Morphology, Organismal Development	abnormal morphology of cerebrum	0,00406		AGA,BDNF,CAV1,FKBP8,GAL,GM2A,PLAUR	7
Cellular Assembly and Organization, Cellular Movement, Nervous System Development and Function	transport of synaptic vesicles	0,00432		CANX,PACSIN1,SNCG,STX7	4
Nervous System Development and Function	sensory system development	0,00493	-0,404	BDNF,GAL,HES1,ID1,S1PR3	5
Cell-To-Cell Signaling and Interaction, Nervous System Development and Function	long-term potentiation of hippocampal cells	0,00508		BDNF,HNRNPK,KCNA4	3
Cellular Development, Embryonic Development, Nervous System Development and Function, Organismal Development, Tissue Development	differentiation of neurosphere cells	0,0058		BDNF,ID2	2
Nervous System Development and Function, Organ Morphology	thickness of cerebral cortex	0,0058		TUBA1A,VIM	2
Cellular Movement, Nervous System Development and Function	migration of neuroglia	0,00583	-1,131	BCR,BDNF,Ccl2,TNC	4
Cellular Assembly and Organization, Cellular Development, Cellular Growth and Proliferation, Nervous System Development and Function, Tissue Development	growth of axons	0,00586	1,498	BDNF,Ccl2,DCLK1,EIF2B2,KIF3C,VIM	6
Cell-To-Cell Signaling and Interaction, Nervous System Development and Function	long-term potentiation	0,00603	1,956	BDNF,GAL,HNRNPK,KCNA4,PLK2,PRKAR1A,TNC,VDAC3	8
Behavior, Nervous System Development and Function	circadian rhythm	0,00634		BHLHE40,ID2,PRKG2,SLC17A6,TNC	5
Cellular Movement, Nervous System Development and Function	migration of interneurons	0,00681		BDNF,PLAUR	2
Nervous System Development and Function	neuroprotection of hippocampus	0,00681		BDNF,PTGS2	2
Cellular Development, Nervous System Development and Function, Tissue Development	differentiation of neuronal progenitor cells	0,00683		BDNF,CAV1,S1PR3	3
Cellular Development, Nervous System Development and Function	development of neuroglia	0,00733		BDNF,EIF2B2,ID2,VIM	4

FIG E4. (Continued).

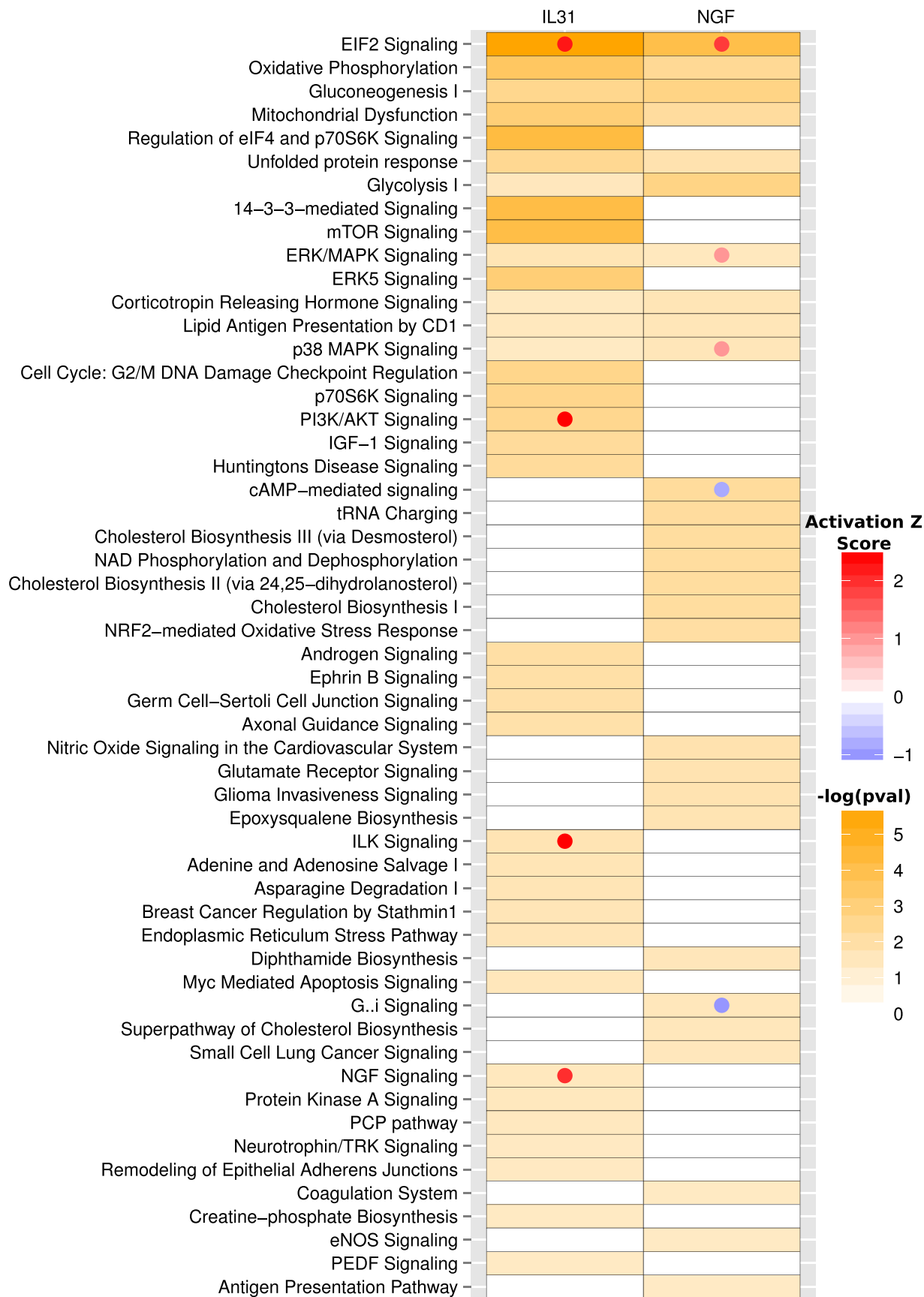


FIG E4. (Continued).

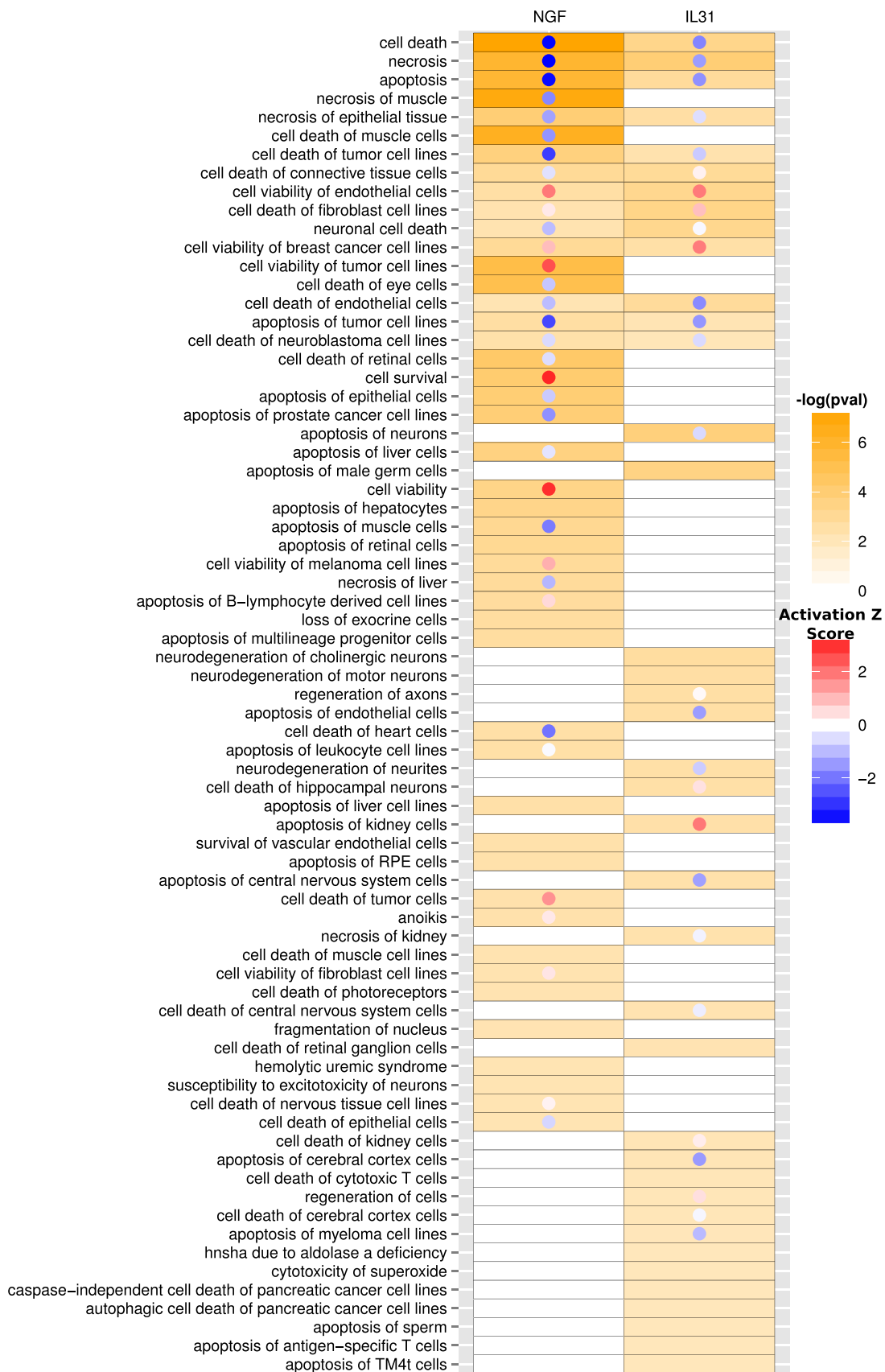


FIG E4. (Continued).



FIG E4. (Continued).

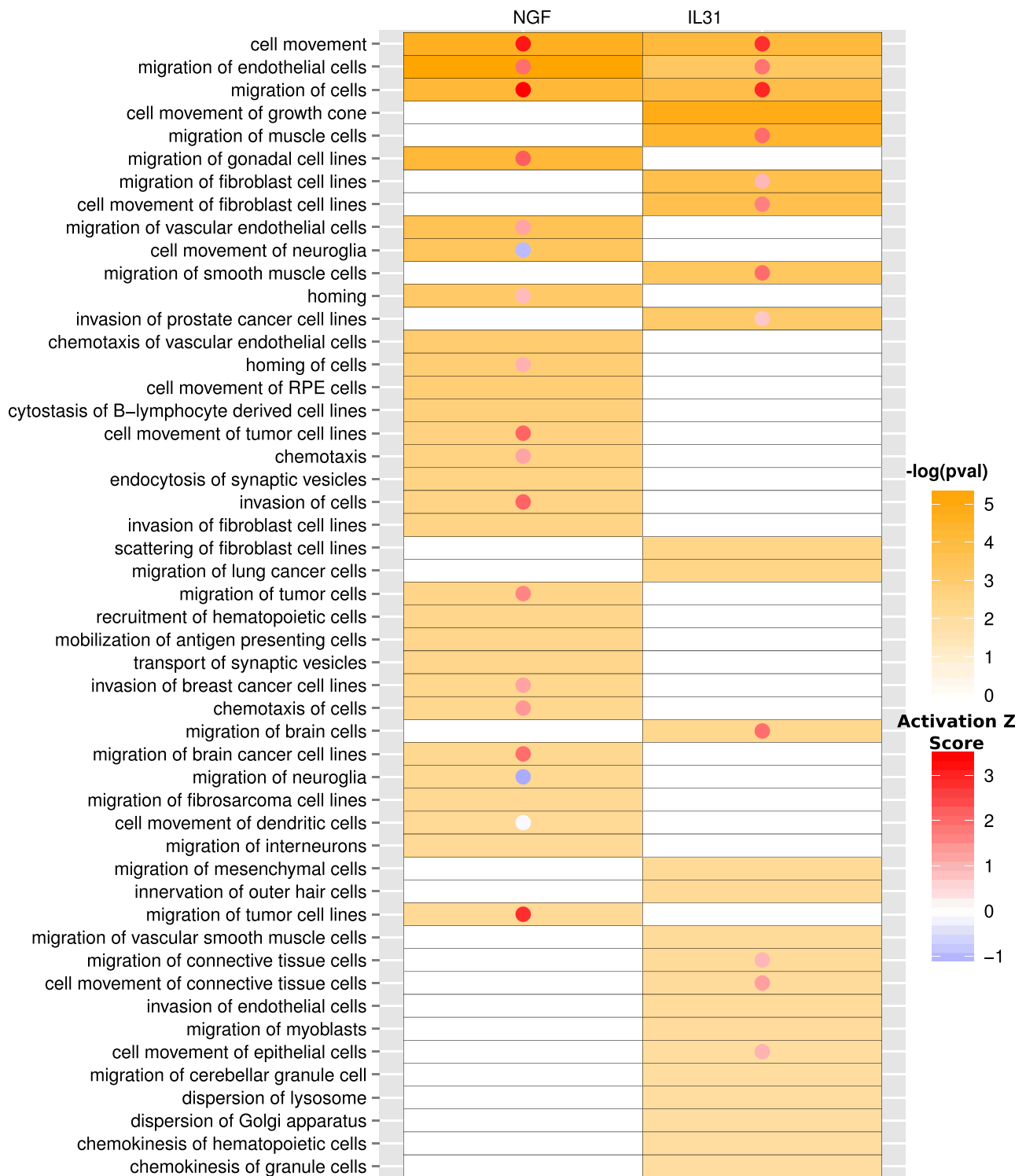


FIG E4. (Continued).

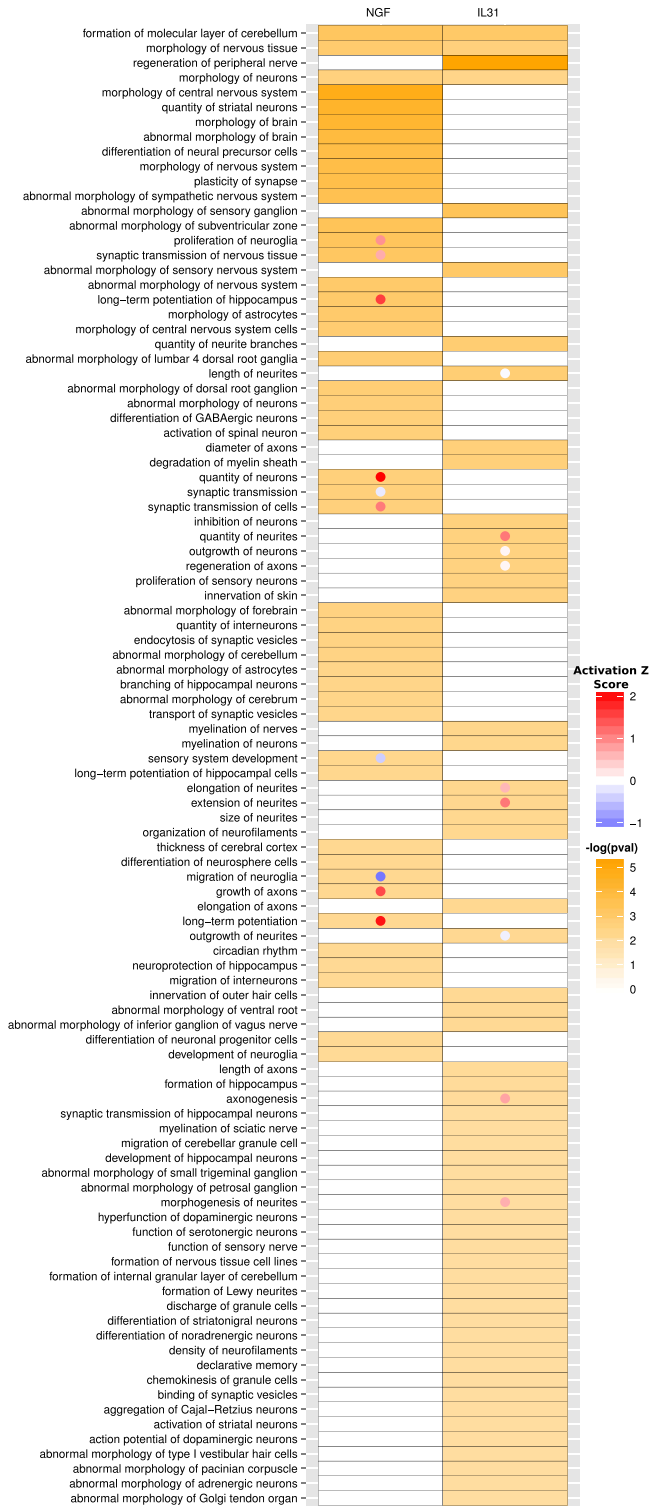


FIG E4. (Continued).